# Lower Jurassic calcareous nannofossil taxonomy revisited according to the Neuquén Basin (Argentina) record

Micaela Chaumeil Rodríguez, Emanuela Mattioli, Juan Pablo Pérez Panera

J. Micropalaeontology, 41, 75–105, 2022
https://doi.org/10.5194/jm-41-75-2022


Journal of Micropalaeontology
Open Access

# Lower Jurassic calcareous nannofossil taxonomy revisited according to the Neuquén Basin (Argentina) record

**Micaela Chaumeil Rodríguez[1,2], Emanuela Mattioli[2,3], and Juan Pablo Pérez Panera[1]**

[1]CONICET – División Científica de Geología, Museo de La Plata,
Paseo del Bosque s/n, La Plata, 1900, Argentina
[2]Univ Lyon, UCBL, ENSL, UJM, CNRS, LGL-TPE, 69622, Villeurbanne, 69100, France
[3]IUF, Institut Universitaire de France, Paris, France

**Correspondence:** Micaela Chaumeil Rodríguez (micachaumeil@gmail.com)

Received: 13 December 2021 – Revised: 17 March 2022 – Accepted: 22 March 2022 – Published: 26 April 2022

**Abstract.** Standard Early Jurassic biostratigraphic studies were performed in the boreal and Tethys realms (western Europe and northern Africa), and biozonations from these areas are the most accurate of the world. Comparatively, investigations in the Pacific realm are scarce, and, in Argentina, they are limited to contributions based on oil-industry subsurface and outcrop reports for the Los Molles Formation. A focused systematic analysis was not previously addressed in the area. The Neuquén Basin in west–central Argentina offers a unique opportunity to study the Early Jurassic calcareous nannofossil history in the south-eastern Pacific Ocean. Calcareous nannofossil assemblages from El Matuasto I section (Los Molles Formation) represent one of the earliest records for the Early Jurassic in the Neuquén Basin and one of the few for the eastern Pacific realm. A detailed systematic analysis allowed the recognition of major bioevents and a comparison with worldwide associations and biostratigraphic schemes. A thorough taxonomic discussion of the Early Jurassic nannofossil species of the Neuquén Basin is presented for the first time. Herein, the taxonomic features of coccoliths recorded in the Neuquén Basin are settled. The age of the calcareous nannofossil assemblages recorded in El Matuasto I is early–late Pliensbachian, covering the NJT4a to NJT4c subzones. Similarities between the Neuquén Basin and localities from the proto-Atlantic region suggest an effective connection between the Pacific and Tethyan basins during the Pliensbachian.

## 1 Introduction

Calcareous nannofossils are remarkable components of Mesozoic marine successions, although their documented distribution may show geographical and temporal biases depending on the discontinuities of the sedimentary record. Classic Lower Jurassic biostratigraphic studies have been primarily built upon locations in the boreal and Tethys realms, namely western Europe and North Africa (e.g. Stradner, 1963; Prins, 1969; Barnard and Hay, 1974; Perch-Nielsen, 1985a; Bown, 1987b; Bown et al., 1988; de Kaenel and Bergen, 1993; de Kaenel et al., 1996; Bown and Cooper, 1998; Mattioli and Erba, 1999; Fraguas et al., 2007, 2015, 2018; Mattioli et al., 2013; Peti et al., 2017; Ferreira et al., 2019). Biozonations from these areas are the most accurate and complete compared to any other part of the world. Several works have been undertaken in Tethyan localities like northern and central Italy (Cobianchi, 1990, 1992; Reale et al., 1992; Baldanza and Mattioli, 1992; Lozar, 1995; Nini et al., 1995; Stoico and Baldanza, 1995; Mattioli, 1996; Picotti and Cobianchi, 1996; Bucefalo Palliani and Mattioli, 1998; Mattioli and Erba, 1999; Cobianchi and Picotti, 2001; Mattioli and Pittet, 2004; Chiari et al., 2007; Bottini et al., 2016), Spain (Perilli, 2000; Tremolada et al., 2005; Fraguas et al., 2007, 2015, 2018; Fraguas and Erba, 2010; Perilli et al., 2010; Sandoval et al., 2012; Menini et al., 2019), Germany (Prins, 1969; Grün et al., 1974; Crux, 1984; Bown, 1987a; Dockerill, 1987; Prins and Driel, 1987; Fraguas et al.,

2013), Portugal (Hamilton, 1977, 1979; Baldanza and Mattioli, 1992; de Kaenel and Bergen, 1996; de Kaenel et al., 1996; Veiga de Oliveira et al., 2007a, b; Suchéras-Marx et al., 2010; Reggiani et al., 2010; López-Otálvaro et al., 2012; Mattioli et al., 2013; Plancq et al., 2016; Ferreira et al., 2019), northern France (Peti et al., 2017), North Africa (de Kaenel and Bergen, 1993; Bodin et al., 2010, 2016; Mercuzot et al., 2019; Baghli et al., 2022), and the United Kingdom (Prins, 1969; Noël, 1972; Rood and Barnard, 1972; Rood et al., 1973; Barnard and Hay, 1974; Moshkovitz, 1979; Hamilton, 1982; Bown, 1987a; Crux, 1987b; Dockerill, 1987; Prins and Driel, 1987; Menini et al., 2021). Taxonomic revisions were also performed, but since Bown (1987b) none of them have dealt with muroliths except Fraguas and Erba (2010).

Comparatively, investigations in the Pacific realm are scarce (Bown, 1987b; Fantasia et al., 2018) and in Argentina are restricted to Los Molles Formation, represented by few general studies (Bown, 1987b, 1992; Ballent et al., 2000, 2011; Angelozzi et al., 2010; Al-Suwaidi et al., 2010, 2016) or contributions based on oil-industry subsurface and outcrop reports (Angelozzi, 1988; Bown and Ellison, 1995; Angelozzi and Ronchi, 2002; Vergani et al., 2003; Angelozzi and Pérez Panera, 2013, 2016; Pérez Panera and Angelozzi, 2015; Gutiérrez Pleimling et al., 2021). However, a focused systematic analysis was not previously addressed in the area.

In this context, the Neuquén Basin, located in west–central Argentina, offers a unique opportunity to study the Early Jurassic calcareous nannofossil history in the south-eastern Pacific Ocean. The basin yields a Lower Jurassic marine transgression from the palaeo-Pacific and records an extensive sedimentary succession (Arregui et al., 2011).

Calcareous nannofossil assemblages from Los Molles Formation represent the earliest record for the Early Jurassic in the Neuquén Basin and one of the few for the eastern Pacific realm (Bown, 1992; Fantasia et al., 2018). This contribution aims at characterizing the Pliensbachian calcareous nannofossil assemblages of the south-eastern Palaeo-Pacific region through a detailed study of El Matuasto I section (Neuquén Basin, Argentina). A detailed systematic analysis allowed recognition of major events and a comparison with worldwide associations and biostratigraphic schemes.

## 2 Geological setting

The Neuquén Basin is located in west–central Argentina, constituting a series of marine and continental sub-basins that have developed behind the Pacific margin of the South American Plate (Fig. 1a) (Legarreta and Uliana, 1999). Since the beginning of the sedimentary filling in the Late Triassic–Early Jurassic, it has accumulated more than 7000 m of Mesozoic deposits (Arregui et al., 2011). During the Pliensbachian–Aalenian interval and in the Tithonian, marine sedimentation was widespread in the Neuquén Basin, while it was restricted to a few areas in other time intervals. Until the Early Cretaceous, this basin was part of the south-eastern Pacific Ocean and had a unique record of marine micro- and macrofossils in the world. The detailed stratigraphic characterizations made on well-exposed outcrops resulted in a thorough understanding of the basin evolution (Groeber, 1918; Weaver, 1931; Stipanicic, 1969; Riccardi, 1983; Gulisano et al., 1984; Legarreta and Gulisano, 1989; Riccardi and Gulisano, 1990; Legarreta and Uliana, 1996, 1999; Lanés, 2005; Leanza, 2009; Arregui et al., 2011; Legarreta and Villar, 2012).

The Los Molles Formation (Weaver, 1931) is mainly composed of grey and dark grey mudstones, with fine to medium sandstones interbedded and variable organic content. Sedimentation corresponds to a marine environment with restricted conditions (Arregui et al., 2011) and represents the earliest Pacific marine transgression in the basin (Legarreta and Uliana, 1996; Legarreta and Villar, 2012). The age of the formation covers the Hettangian to Callovian, considering its total extension in the different areas of the basin (Gulisano and Gutiérrez Pleimling, 1995; Vergani et al., 1995; Legarreta and Uliana, 1996; Cruz et al., 1999; Veiga et al., 2009; Riccardi, 2008a; Arregui et al., 2011; Legarreta and Villar, 2012; Spalletti et al., 2012; Sales et al., 2014; Casadío and Montagna, 2015).

The El Matuasto I section is located approximately 45 km south of the city of Zapala (Neuquén Province) and 1 km from the Picún Leufú River bridge along the Ruta Nacional 40 (Fig. 1b–c). It is represented by a 33 m thick succession of mudstones with thin fine–medium sandstone intercalations. Sand beds are interpreted as turbidites, where the basin experienced episodes of continental sediment input. Bioturbation and plant debris are common throughout the sequence.

## 3 Materials and methods

A set of 26 samples from the El Matuasto I section (Los Molles Formation) was analysed for calcareous nannofossils. The preparation method consists of a slight modification of the technique described by Beaufort et al. (2014). A small amount of powdered rock was diluted with 30 mL of water. The suspension was poured on a coverslip in a Petri dish. The cover slide was weighed before applying the suspension with the study material. Once the sediment was settled (after 4 h), the water was carefully removed to avoid turbulence. The coverslip was then dried to remove the remaining water, weighed again, and then mounted on a microscope slide using Norland 61 optical glue. This method enables us to calculate the absolute abundance (nannofossil per gram of sediment) using the formula described by Menini et al. (2019).

Identification and counting of calcareous nannofossils were performed using a Leica DMP 750 petrographic microscope at 1000× magnification under crossed polars. Photographs were taken with a Leica MC 170 HD camera. For each sample 300 specimens were counted, thus ensuring that

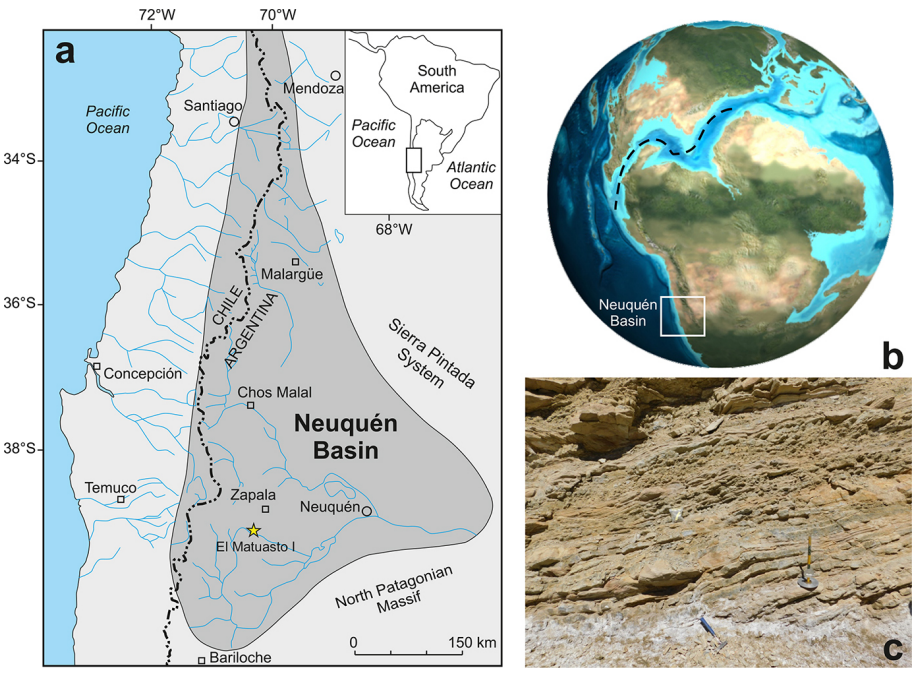


**Figure 1.** **(a)** Geographical setting of the Neuquén Basin and the El Matuasto I section (Argentina) (adapted after Howell et al., 2005). **(b)** Palaeogeographic reconstruction for the Early Jurassic showing the possible connection between the Pacific and Tethys oceans during the Pliensbachian (adapted after Global Paleogeography, http://plate-tectonic.narod.ru/globalpaleogeophotoalbum.html, last access: 12 March 2022). **(c)** View of the El Matuasto I section, Los Molles Formation.

the probability of not recovering a rare species is below 5 % (Fatela and Taborda, 2002). In the slides for which a low nannofossil abundance made it difficult to count 300 specimens, the counting stopped at 450 fields of view (FOV; the area of one FOV is 0.0069 $mm^2$).

All nannofossil data were integrated in a distribution chart (Fig. 2). The absolute abundance (as nannofossils per gram of sediment) and preservation index are also indicated. Preservation is a discrete scale based on the general aspect of the specimens (Roth, 1984). G: good – most specimens exhibit little or no secondary alterations and delicate structures such as spines are preserved in most cases. M: moderate – specimens exhibit some degree of overgrowth and/or dissolution (identification of species not compromised). P: poor – the effects of overgrowth and/or dissolution are very intense (identification of species is impaired but possible in some cases).

The systematic palaeontology follows the criteria by de Vargas et al. (2007) for subclass level and up and Young and Bown (1997) and Bown and Young (1997) for levels below subclass.

For biostratigraphic analysis, the following nannofossil events are used after Gradstein et al. (2012): FO (first occurrence), LO (last occurrence), LCO (last common occurrence). They are correlated with the biozones of Bown et al. (1988), Bown and Cooper (1998), de Kaenel and Bergen (1993), Mattioli and Erba (1999), and Ferreira et al. (2019); they appear in the text as NJ (Nannofossil Jurassic) and NJT (Nannofossil Jurassic Tethyan) zones. Standard and Neuquén Basin Ammonite Zonations (SAZ and NAZ, respectively) (Riccardi, 2008b) are correlated with these nannofossil biozones.

## 4 Results

A total of 16 samples of the El Matuasto I section yielded calcareous nannofossils, while 10 were barren. The general preservation of the assemblage is moderate to good, with overall better preservation towards the upper part of the section. Sample richness varies between a minimum of 10 and a maximum of 18 species per sample. Stratigraphic distribution of nannofossils and other features are given in Fig. 2.

For all the recovered species, the entire synonymies provided in the literature, the original papers describing the holotype, and the available literature illustrating a given species were carefully checked. The systematic palaeontology below is thus based upon a careful revisitation of previous literature and presents a synonymy list as complete as possible. For each species, remarks are provided with respect to the original diagnosis, which also make reference to descriptions provided in the literature.

As far as the coccolith morphology is concerned, we refer to Young (1992) for the murolith and placolith description and to Bown (1987b) for the protolith and loxolith structure. The protolith rim structure of muroliths comprises a domi-

**Calcareous Nannofossils Distribution Chart**
**El Matuasto I Section**

| System | Series | Stage | Sample | Fields of View | Total specimens | Preservation | Abundance (n/FoV) | Abundance (n/s) | Richness | Diversity (Shannon index) | ***Biscutum grande*** | *Calyculus* aff. *cribrum* | *Crepidolithus crassus* | *Crepidolithus crucifer* | *Crepidolithus granulatus* | *Crepidolithus impontus* | *Crepidolithus pliensbachensis* | *Crepidolithus timorensis* | *Crucirhabdus primulus* | ***Lotharingius barozii*** | *Mitrolithus elegans* | *Mitrolithus lenticularis* | *Parhabdolithus liasicus distinctus* | *Parhabdolithus liasicus liasicus* | *Parhabdolithus robustus* | ***Similiscutum cruciulus* group** | ***Similiscutum finchii*** | large *Similiscutum* aff. *finchii* | *Tubirhabdus patulus* thick | *Tubirhabdus patulus* thin | *Schizosphaerella* (fragment) | Nanofossil Tethyan Subzones Ferreira et al. (2019) |
|---|---|---|---|---|---|---|---|---|---|---|---|---|---|---|---|---|---|---|---|---|---|---|---|---|---|---|---|---|---|---|---|---|
| Jurassic | Early Jurassic | Upper Pliensbachian | EM-I-26 | 83 | 299 | M/G | 3,6 | 1,6E+08 | 15 | 2,2 | | | 4 | | 4 | 16 | | | 19 | | 7 | 10 | 75 | 9 | 11 | 12 | 4 | 7 | 85 | 33 | 3 | NJT4c |
| | | | EM-I-25 | 300 | 326 | M/G | 1,1 | 3,6E+07 | 18 | 2,6 | 3 | | 8 | | 12 | 13 | 1 | | 18 | 16 | 9 | 14 | 67 | 12 | 21 | 32 | 3 | 2 | 33 | 51 | 11 | |
| | | | EM-I-24 | 27 | 307 | G | 11,4 | 2,4E+08 | 15 | 2,4 | 2 | | 9 | | 7 | 17 | | | 25 | 43 | 19 | | 68 | 13 | 15 | 9 | 2 | | 28 | 43 | 7 | |
| | | | EM-I-23 | 34 | 300 | M | 8,8 | 1,0E+08 | 17 | 2,5 | 4 | 3 | 18 | | 10 | 12 | | | 3 | 81 | 12 | 3 | 26 | | 7 | 47 | 6 | 7 | 18 | 39 | 4 | |
| | | | EM-I-22 | 450 | N/A | N/A | N/A | N/A | N/A | N/A | | | | | | | | | | | | | | | | | | | | | | |
| | | | EM-I-21 | 450 | 74 | P | 0,2 | 4,2E+06 | 11 | 1,7 | 42 | | 3 | | 1 | | | | | | 3 | 6 | 3 | | | 4 | | 1 | 3 | 5 | 3 | |
| | | | EM-I-20 | 450 | N/A | N/A | N/A | N/A | N/A | N/A | | | | | | | | | | | | | | | | | | | | | | |
| | | | EM-I-19 | 43 | 310 | M/G | 7,2 | 1,7E+08 | 15 | 2,1 | 14 | 1 | 53 | | 28 | 105 | | | 11 | 3 | | 3 | 31 | 2 | 17 | 6 | | | 15 | 16 | 5 | |
| | | | EM-I-18 | 57 | 377 | M/G | 6,6 | 1,3E+08 | 17 | 2,3 | 30 | 4 | 76 | | 78 | 52 | 1 | | 7 | 4 | 4 | 6 | 35 | 5 | 16 | 19 | | | 14 | 23 | 3 | |
| | | | EM-I-17 | 450 | N/A | N/A | N/A | N/A | N/A | N/A | | | | | | | | | | | | | | | | | | | | | | |
| | | | EM-I-16 | 450 | 243 | P/M | 0,5 | 1,0E+07 | 14 | 2,0 | 13 | 4 | 98 | 2 | 14 | 28 | 1 | | 2 | | | 8 | 38 | | 4 | | | | 5 | 15 | 11 | |
| | | | EM-I-15 | 450 | 267 | P/M | 0,6 | 1,1E+07 | 13 | 2,1 | 27 | | 62 | | 6 | 36 | | | 7 | 5 | | 6 | 27 | 3 | 3 | | | | 10 | 68 | 7 | |
| | | Lower Pliensbachian | EM-I-14 | 450 | 242 | P/M | 0,5 | 2,3E+07 | 12 | 1,9 | 3 | | 38 | | 10 | 12 | | | 3 | | 7 | | 24 | 5 | 4 | | | | 39 | 92 | 5 | NJT4b |
| | | | EM-I-13 | 178 | 301 | P/M | 1,7 | 5,1E+07 | 14 | 2,2 | 2 | | 51 | | 12 | 35 | | 4 | 10 | | 7 | 7 | 29 | 5 | 12 | | | | 43 | 75 | 9 | |
| | | | EM-I-12 | 206 | 300 | P/M | 1,5 | 3,9E+07 | 14 | 2,3 | 27 | | 45 | | 23 | 67 | | | 6 | | 11 | 2 | 36 | 3 | 10 | 2 | | | 32 | 17 | 19 | |
| | | | EM-I-11 | 150 | 345 | P/M | 2,3 | 7,3E+07 | 14 | 2,4 | 3 | | 45 | | 27 | 40 | | | 21 | | 23 | 14 | 42 | 11 | 29 | 5 | | | 40 | 37 | 8 | |
| | | | EM-I-10 | 450 | 36 | P/M | 0,1 | 1,5E+06 | 10 | 1,8 | | | 2 | | | 9 | | | 3 | | 1 | 2 | 13 | 1 | 3 | | | | | 1 | 1 | |
| | | | EM-I-9 | 450 | 76 | P/M | 0,2 | 1,7E+06 | 11 | 2,1 | | 6 | 11 | | | 13 | | | 3 | | 4 | 14 | 3 | | 4 | | | | 1 | 1 | 16 | |
| | | | EM-I-8 | 450 | N/A | N/A | N/A | N/A | N/A | N/A | | | | | | | | | | | | | | | | | | | | | | |
| | | | EM-I-7 | 450 | N/A | N/A | N/A | N/A | N/A | N/A | | | | | | | | | | | | | | | | | | | | | | |
| | | | EM-I-6 | 450 | N/A | N/A | N/A | N/A | N/A | N/A | | | | | | | | | | | | | | | | | | | | | | |
| | | | EM-I-5 | 450 | N/A | N/A | N/A | N/A | N/A | N/A | | | | | | | | | | | | | | | | | | | | | | |
| | | | EM-I-4 | 450 | N/A | N/A | N/A | N/A | N/A | N/A | | | | | | | | | | | | | | | | | | | | | | |
| | | | EM-I-3 | 450 | N/A | N/A | N/A | N/A | N/A | N/A | | | | | | | | | | | | | | | | | | | | | | |
| | | | EM-I-2 | 450 | N/A | N/A | N/A | N/A | N/A | N/A | | | | | | | | | | | | | | | | | | | | | | |
| | | | EM-I-1 | 450 | 164 | M | 0,4 | 7,6E+06 | 11 | 2,1 | | | 30 | 1 | 5 | | | | 10 | | 25 | 30 | 27 | 3 | | 1 | | | 15 | | 17 | |

**Figure 2.** Distribution chart of calcareous nannofossils from El Matuasto I, Los Molles Formation. Preservation index: P (poor), M (moderate), G (good), N/A (not applicable); grey cell (barren). Abundance (n/FoV): nannofossils per field of view. Abundance (n/s): nannofossils per gram of sediment. Biozones consigned after Ferreira et al. (2019). Marker species in bold.

nant distal shield and a proximal shield, both showing a vertical (distal) extension (see Bown, 1987b, text-fig. 6B). The distal shield is composed of elements joined along sutures which are perpendicular to the coccolith base without imbrication. The protolith rim structure is possessed by the genera *Crucirhabdus*, *Mitrolithus*, and *Parhabdolithus*. The loxolith rim structure of muroliths comprises a dominant distal shield and a proximal shield with a vertical (distal) extension (see Bown, 1987b, text-fig. 6A). The distal shield is composed of tall, narrow, steeply inclined and imbricating laths. The loxolith rim is possessed by the genera *Crepidolithus* and *Tubirhabdus*. The placolith rim structure possesses elements forming a slightly concave–convex shield developing in the horizontal plane parallel to the cell surface as opposed to the murolith tall upright rims, which were vertically orientated. The radiating placolith rim structure comprises a proximal and distal shield, both unicyclic (Bown, 1987b, text-fig. 7A). The distal shield is composed of blade-like laths lying side by side, with the suture lines between each element orientated radially to the central area of the coccolith. The genera which display this structure include *Biscutum*, *Similiscutum*, and *Calyculus*. The imbricating placolith rim structure consists of a bicyclic distal shield, a unicyclic proximal shield, and a connecting inner wall (Bown, 1987b, text-fig. 7B). The distal shield outer cycle is composed of blade-like laths which are imbricating and joined along sutures with anti-clockwise inclination. The only genus considered here which displays this structure is *Lotharingius*.

### 4.1 Systematic palaeontology

Division HAPTOPHYTA Hibberd ex Edvardsen and Eikrem in Edvardsen et al., 2000

Class PRYMNESIOPHYCEAE Hibberd, 1976; emend. Cavalier-Smith in Cavalier-Smith et al., 1996

Subclass CALCIHAPTOPHYCIDAE de Vargas et al., 2007

Grade "HETEROCOCCOLITHS" Braarud et al., 1955a, b

Order EIFFELLITHALES Rood et al., 1971

Family CHIASTOZYGACEAE Rood et al., 1973 emend. Varol and Girgis, 1994

Genus ***Crepidolithus*** Noël, 1965b

*Type species*. *Crepidolithus crassus* (Deflandre in Deflandre and Fert, 1954) Noël, 1965b

***Crepidolithus crassus*** (Deflandre in Deflandre and Fert, 1954) Noël, 1965b
(Plate 1, figs. 1–2)

1954 *Discolithus crassus* Deflandre in Deflandre and Fert, p. 144, pl. 15, figs. 12–13, text-fig. 49.
1965a *Crepidolithus crassus* (Deflandre, 1954); Noël, p. 5, text-figs. 17–21.
1965b *Crepidolithus crassus* (Deflandre, 1954); Noël, pl. 2, figs. 3–7; pl. 3, fig. 1–5; text-figs. 17–21.
non 1969 *Crepidolithus crassus* (Deflandre, 1954) Noël, 1965b. Prins, pl. 1, fig. 5C.
1973 *Crepidolithus crucifer* Prins, 1969; Rood et al., pl. 2, fig. 4.
1979 *Crepidolithus crassus* (Deflandre, 1954) Noël, 1965b. Goy in Goy et al., 1979, pl. 2, fig. 1.
non 1979 *Crepidolithus crassus* (Deflandre, 1954) Noël, 1965b. Medd, p. 54, pl. 1, figs. 7–8.
1981 *Crepidolithus crassus* (Deflandre, 1954) Noël, 1965b. Goy, pl. 5, figs. 8, 10–11 (non fig. 9); pl. 6, fig. 1.
1982 *Crepidolithus crassus* (Deflandre, 1954) Noël, 1965b. Hamilton in Lord, pl. 3.1, fig. 4 (non fig. 3).
non 1986 *Crepidolithus crassus* (Deflandre, 1954) Noël, 1965b. Young et al., pl., fig. M.
1987a *Crepidolithus crassus* (Deflandre, 1954) Noël, 1965b. Bown, pl. 1, figs. 1–2.
1987b *Crepidolithus crassus* (Deflandre, 1954) Noël, 1965b. Bown, pp. 16–17, pl. 1, figs. 6–11; pl. 12, figs. 5–6.
1988 *Crepidolithus crassus* (Deflandre, 1954) Noël, 1965b. Angelozzi, p. 142, pl. 2, figs. 4–5.
1992 *Crepidolithus pliensbachensis* (Crux, 1985) Bown, 1987b. Cobianchi, fig. 22i–l.
1994 *Crepidolithus crassus* (Deflandre, 1954) Noël, 1965b. Goy et al., pl. 7, figs. 3–4.
1998 *Crepidolithus timorensis* (Kristan-Tollmann, 1988a) Bown in Bown and Cooper, pl. 4.9, figs. 13–14 (= small *C. crassus*).
1998 *Crepidolithus crassus* (Deflandre, 1954) Noël, 1965b. Bown and Cooper in Bown, pl. 4.1, fig. 1; pl. 4.9, figs. 1–2.
1998 *Crepidolithus crassus* (Deflandre, 1954) Noël, 1965b. Parisi et al., pl. 4, fig. 2.
1999 *Crepidolithus crassus* (Deflandre, 1954) Noël, 1965b. Mattioli and Erba, p. 364–365, pl. 1, fig. 8, tex–fig. 8.
2000 *Crepidolithus crassus* (Deflandre, 1954) Noël, 1965b. Walsworth-Bell, p. 51, fig. 4.7; p. 90, fig. 6.3.
2007 *Crepidolithus crassus* (Deflandre, 1954) Noël, 1965b. Fraguas et al., p. 232–233, pl. 1, fig. 1.
2008 *Crepidolithus crassus* (Deflandre, 1954) Noël, 1965b. Aguado et al., fig. 5.11–12.
2008 *Crepidolithus crassus* (Deflandre, 1954) Noël, 1965b. Fraguas et al., pl. 1, fig. 1.
2010 *Crepidolithus crassus* (Deflandre, 1954) Noël, 1965b. Reggiani et al., pp. 2–3, pl. 1, figs. 3–6.
2010 "small *crassus*" Suchéras-Marx et al., fig. 7.
2013 *Crepidolithus crassus* (Deflandre, 1954) Noël, 1965b. Mattioli et al., pl. 1, fig. 14.
2014 *Crepidolithus cantabriensis*. Fraguas, fig. 3f (non figs. 3a–e).
2015 *Crepidolithus crassus* (Deflandre in Deflandre and Fert, 1954) Noël, 1965b. Casellato and Erba, pl. 1.18–19, and "small" *C. crassus* pl. 1.20.
2017 *Crepidolithus crassus* (Deflandre in Deflandre and Fert, 1954) Noël, 1965b. Peti et al., fig. 5I; figs. S.2 34–35 (appendix F).
2019 *Crepidolithus crassus* (Deflandre in Deflandre and Fert, 1954) Noël, 1965b. Menini et al., p. 16, pl. 1., figs. 4–5.
2019 *Crepidolithus crassus* (Deflandre in Deflandre and Fert, 1954) Noël, 1965b. Ferreira et al., p. 8, pl. 1, fig. 21.
2021 *Crepidolithus crassus* (Deflandre in Deflandre and Fert, 1954) Noël, 1965b. Fraguas et al., fig. 9, CM.249.

*Range*. Sinemurian–Tithonian (Bown and Cooper, 1998).

*Occurrence*. Given the wide range of *C. crassus*, this species has been recorded in the entire studied interval. The FO of this species is used by some authors to mark the NJ2–NJ3 zone boundary (Barnard and Hay, 1974; Bown and Cooper, 1998; Fraguas et al., 2015).

*Remarks*. The original diagnosis of *Discolithus crassus* describes an "elliptical slightly elongated, thick coccolith without an elevated rim, exhibiting an undulated longitudinal median line, interrupted in its centre by divergent lateral lines and few punctuations (? perforations)" (Deflandre in Deflandre and Fert, 1954, pp. 115–176). Noël (1965b, p. 88) emended this diagnosis, stating that it is "a typical *Crepidolithus*". The punctuation reported by Deflandre and Fert (1954) might be the result of poor preservation of the specimen that they illustrate under light microscope (LM). The later description by Bown (1987b; p. 16) reports a "broad, high, elliptical rim with a vacant central area often reduced to a lenticular slit… The broader the wall the narrower the central area". Actually, scanning electron microscope (SEM) pictures (Bown, 1987b, pl. 1, figs. 6–9, p. 15) show a variable-sized, vacant central area. In fact, Noël (1965b) and Bown (1987b) observed a certain variability in the central area of *C. crassus*, which can be slightly open. Suchéras-Marx et al. (2010) reported two different-sized coccolith morphotypes, named "small *crassus*" with a mean size of 6.5 µm and "large *crassus*" with a mean size of 8.5 µm. Fraguas and Erba (2010) performed biometric analysis on *C. crassus* and *C. crucifer*, and they differentiated the

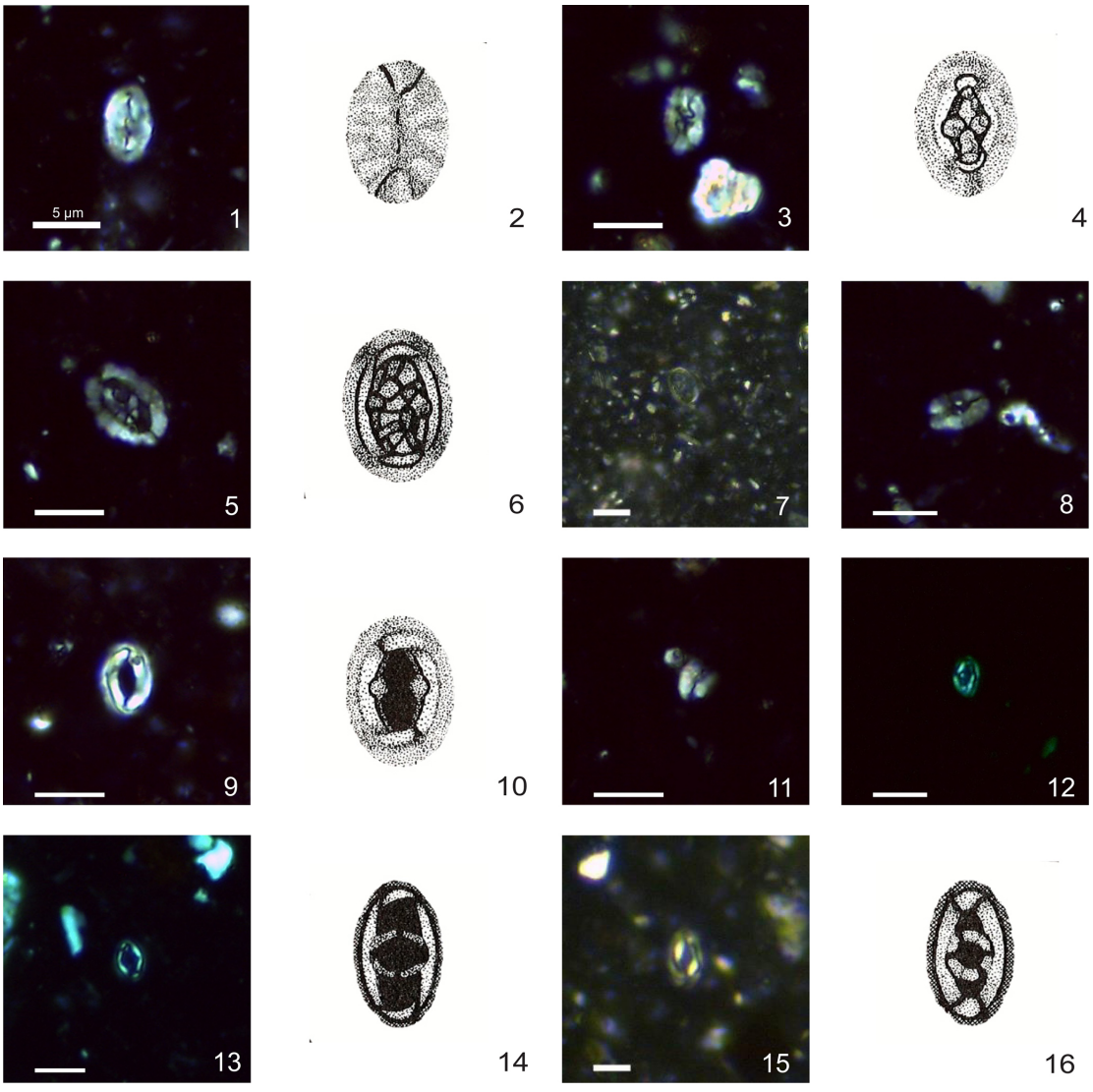


**Plate 1.** Calcareous nannofossils from El Matuasto I, Los Molles Formation, Neuquén Basin. All pictures from LM under crossed nicols and distal view unless specified. Scale bar: 5 µm. All illustrations adapted after Prins (1969). **(1, 2)** *Crepidolithus crassus* (Deflandre in Deflandre and Fert, 1954) Noël, 1965b, EM-I-18 (YT.RMP_N.000012.10). **(3, 4)** *Crepidolithus crucifer* Prins ex Rood et al., 1973 emend. Fraguas and Erba, 2010, EM-I-16 (YT.RMP_N.000012.9). **(5, 6)** *Crepidolithus granulatus* Bown, 1987b, thick morphotype, EM-I-12 (YT.RMP_N.000012.5). **(7)** *Crepidolithus granulatus* Bown, 1987b, thin morphotype, EM-I-11 (YT.RMP_N.000012.4). **(8)** *Crepidolithus pliensbachensis* (Crux, 1985) emend. Bown, 1987b, EM-I-16 (YT.RMP_N.000012.9). **(9)** *Crepidolithus impontus* Grün, Prins and Zweili, 1974, EM-I-10 (YT.RMP_N.000012.3). **(10)** *Crepidolithus impontus* Grün, Prins and Zweili, 1974, slightly tilted, EM-I-19 (YT.RMP_N.000012.11). **(11)** *Crepidolithus timorensis* (Kristan-Tollmann, 1988a) Bown in Bown and Cooper, 1998, EM-I-13 (YT.RMP_N.000012.6). **(12)** *Tubirhabdus patulus* Prins, 1969 ex Rood et al., 1973, tiny morphotype, EM-I-1 (YT.RMP_N.000012.1). **(13, 14)** *Tubirhabdus patulus* Prins, 1969 ex Rood et al., 1973, thin morphotype, EM-I-11 (YT.RMP_N.000012.4). **(15, 16)** *Tubirhabdus patulus* Prins, 1969 ex Rood et al., 1973, thick morphotype, EM-I-10 (YT.RMP_N.000012.3).

two species on the basis of biometry, concluding that *C. crassus* has a smaller size (mean size 6.91 µm) than *C. crucifer* (mean size 8.96 µm) (see Fig. 3). Despite the small average size of *C. crassus* reported by Fraguas and Erba (2010), the measured specimens virtually integrate both the small *crassus* and large *crassus* of Suchéras-Marx et al. (2010). In fact, the differences between *C. crassus* and *C. crucifer* also concern the central-area structures.

***Crepidolithus crucifer*** Prins ex Rood et al., 1973 emend. Fraguas and Erba, 2010
(Plate 1, figs. 3–4)

1969 *Crepidolithus crucifer* Prins, p. 551, pl. 1, fig. 3a (non fig. b) (nomen nudum).
non 1973 *Crepidolithus crucifer* Prins, 1969. Rood et al., p. 374, pl. 2, fig. 4.
1974 *Crepidolithus crucifer* Prins ex Rood et al., 1973. Barnard and Hay, pl. 1, fig. 5; pl. 4, fig. 5.
1977 *Crepidolithus crucifer* Prins ex Rood et al., 1973. Hamilton, pp. 586, pl. 3, fig. 10.
1978 *Crepidolithus crucifer* Prins ex Rood et al., 1973. Hamilton, pp. 183–184, pl. 7, fig. 2.
1979 *Crepidolithus crassus* (Deflandre, 1954) Noël, 1965b. Medd, p. 54, pl. 1, fig. 8 (non fig. 7).
1981 *Crepidolithus crassus* (Deflandre, 1954) Noël, 1965b; Goy, pl. 5, fig. 9 (non figs. 8, 10–11).
1982 *Crepidolithus crucifer* Prins ex Rood et al., 1973. Hamilton in Lord, pl. 3.1, fig. 1.
?1986 *Crepidolithus crassus* (Deflandre, 1954) Noël, 1965b. Young et al., pl., fig. M.
1992 *Crepidolithus cavus* Prins ex Rood et al., 1973. Cobianchi, fig. 22h.
1994 *Crepidolithus* sp. Noël, 1973. Gardin and Manivit, p. 230–231, pl. 1, figs. 13–14.
2003 *Crepidolithus crassus* (Deflandre, 1954) Noël, 1965b. Asgar-Deen et al., pp. 58–59, fig. 11, text-fig. 11.
2010 *Crepidolithus crucifer* Prins ex Rood et al., 1973 emend. Fraguas and Erba, p. 134, fig. 3b.
2015 *Crepidolithus granulatus* Bown, 1987b. Casellato and Erba, pl. 1.22.
2019 *Crepidolithus crucifer* Prins, 1969. Menini et al., p. 16, pl. 1, fig. 12.
2019 *Crepidolithus crucifer* Prins, 1969. Ferreira et al., p. 8, pl. 1, fig. 22.

*Range*. Pliensbachian (Fraguas and Erba, 2010).

*Occurrence*. This species has been recorded in the entire studied interval.

*Remarks*. This species was introduced by Prins (1969) as nomen nudum. Prins (1969) showed a drawing in which a thick cross spanned a narrow central area, and the cross is composed of granular calcite crystals. Rood et al. (1973) provided a SEM picture showing a *Crepidolithus* in proximal view with a very reduced central area without visible structure, as well as a description stating, "a species of *Crepidolithus* with a cruciform structure in the central area" (p. 374). According to the latter, Bown (1987b) put *C. crucifer* in synonymy with *C. crassus*. However, *C. crassus* possesses a vacant central area. Thus, the presence of a cruciform structure in the central area of *C. crucifer* represents a valuable morphological difference between the two species. Moreover, Fraguas and Erba (2010) nicely illustrated by means of SEM and biometry that *C. crassus* and *C. crucifer* can be clearly differentiated. They provided an emended diagnosis: "A robust, thick and elliptical species of *Crepidolithus* with a relatively narrow and large central area filled by a structure consisting of a cross aligned along the major and minor axes of the ellipse that sometimes appears weakly developed" (p. 134). Although they include the presence of a cross aligned to the major and minor axes of the ellipse, in their picture (fig. 3b) the cross is not visible but a coarse granulation. In their description they stated that the central-area structure often appears as irregular grains. This peculiar morphology is also visible in the SEM picture of *C. crucifer* showed by Barnard and Hay (1974) (although broken) and in the Medd (1979) *C. crassus* (see Fig. 3). Other characteristics allowing a differentiation of *C. crucifer* from *C. crassus* are a bigger size for *C. crucifer* (Fraguas and Erba, 2010) and the fact that the elements of the distal shield appear quite large, providing an irregular outline under LM.

***Crepidolithus granulatus*** Bown, 1987b

*Range*. Pliensbachian–Toarcian, Early Jurassic (Bown and Cooper, 1998).

*Occurrence*. Both morphotypes of this species have been recorded in the entire studied interval.

*Remarks*. This elliptical coccolith has a low distal rim and a large, wide central area filled with small, granular calcite crystals. Bown (1987b) explains that this species shows variable thickness of the distal shield, and, as a consequence, the central-area opening can be more or less developed. This difference is figured in many previous publications (Mattioli et al., 2013; Peti et al., 2017). *Crepidolithus granulatus* is herein presented as two morphotypes described separately below. The rim thickness variation reflects likely a palaeoenvironmental or palaeogeographical control, but further biometric study is necessary to better constrain the differences between the two morphotypes.

***Crepidolithus granulatus*** Bown, 1987b (thick morphotype)
(Plate 1, figs. 5–6)

1977 *Ethmorhabdus* aff. *E. gallicus* Noël, 1965b. Hamilton, pl. 1, fig. 6.
1981 *Crepidolithus impontus* Goy, pl. 6, figs. 7–8.
1984 *Crepidolithus crassus* (Deflandre in Deflandre and Fert, 1954) Noël, 1965b. Crux, fig. 11.1.
1987b *Crepidolithus granulatus* Bown, p. 17, pl. 1, figs. 14–15; pl. 12, figs. 1, 5.
1998 *Crepidolithus granulatus* Bown, 1987b. Bown and Cooper in Bown, pl. 4.1, figs. 2–3; pl. 4.9, fig. 3.
2007a *Crepidolithus granulatus* Bown, 1987b. Veiga de Oliveira et al., fig. 5.P.
2007b *Crepidolithus granulatus* Bown, 1987b. Veiga de Oliveira et al., fig. 1.
2013 large *Crepidolithus granulatus* Bown, 1987b. Mattioli et al., pl. 1.15.

non 2013 *Crepidolithus granulatus* Bown, 1987b. Rai and Jain, pl. 2, figs. 2a–c; pl. 3, figs. 3a–c.
2014 *Crepidolithus granulatus* Bown, 1987b. Reolid et al., fig. 6 (thick).
non 2015. *Crepidolithus granulatus* Bown, 1987b. Casellato and Erba, pl. 1.22.
non 2016. *Crepidolithus granulatus* Bown, 1987b. Rai et al., fig. 2.19a–b.
2019 *Crepidolithus granulatus* Bown, 1987b. Menini et al., pl. 1.
2019 *Crepidolithus granulatus* Bown, 1987b. Ferreira et al., pl. 1 (Peniche74).

*Remarks*. Coccoliths displaying a thick distal shield and a wide central area filled with slightly disorganized bulky calcite crystals. Usually, the central boss is not recognizable.

***Crepidolithus granulatus*** Bown, 1987b (thin morphotype) (Plate 1, fig. 7)

1969 *Crepidolithus crassus* (Deflandre, 1954) Noël, 1965b. Prins, pl. 1, fig. 5C.
1977 *Ethmorhabdus* aff. *E. gallicus* Noël, 1965b. Hamilton, pl. 1, figs. 4–5.
1984 *Crepidolithus crassus* (Deflandre in Deflandre and Fert, 1954) Noël, 1965b. Crux, fig. 11.2.
1987b *Crepidolithus granulatus* Bown, p. 17, pl. 1, figs. 12–13.
1998 *Crepidolithus granulatus* Bown, 1987b. Bown and Cooper in Bown, pl. 4.9, figs. 4–5.
2006 *Crepidolithus granulatus* Bown, 1987b. Perilli and Duarte, pl. 1, fig. 15.
2010 *Crepidolithus granulatus* Bown, 1987b. Reggiani et al., pl. 1, figs. 7–8.
2014 *Crepidolithus granulatus* Bown, 1987b. Reolid et al., fig. 6 (thin).
2015 *Crepidolithus cavus* Prins ex Rood et al., 1973. Casellato and Erba, pl. 1.21.
2017 *Crepidolithus granulatus* Bown, 1987b. Peti et al., fig. 5K; fig. S.2 22 (appendix F).
2019 *Crepidolithus granulatus Bown*, 1987b. Ferreira et al., pl. 1 (Peniche97).

*Remarks*. Specimens with a thin distal rim and a wide central area filled with small calcite crystals where a small boss is distinguishable.

***Crepidolithus impontus*** Grün, Prins and Zweili, 1974 (Plate 1, figs. 9–10)

non 1969 *Crepidolithus cavus* Prins, pl. 1, fig. 4C (nomen nudum).
1974 *Crepidolithus cavus* Prins, 1969 ex Rood et al., 1973. Barnard and Hay, pl. 1, fig. 2.
1974 *Crepidolithus impontus* Grün, Prins and Zweili, pp. 310–311, pl. 2, figs. 1–3.
1978 *Crepidolithus cavus* Prins, 1969 ex Rood et al., 1973. Hamilton, pl. 7, fig. 3.
1979 *Crepidolithus impontus* Grün, Prins and Zweili, 1974 emend. Goy in Goy et al., p. 39, pl. 2, fig. 2.
1981 *Crepidolithus impontus* Grün, Prins and Zweili, 1974; Goy, pp. 28–29, pl. 6, figs. 2–6 (non figs. 7–8); pl. 7, fig. 1. text-fig. 5.
1982 *Crepidolithus cavus* Prins, 1969 ex Rood et al., 1973. Hamilton in Lord, pl. 3.1, fig. 2.
1987b *Crepidolithus cavus* Prins ex Rood et al., 1973. Bown, pp. 13–16, pl. 1, figs. 4–5; pl. 12, figs. 3–4.
1998 *Crepidolithus impontus* (Grün et al., 1974) Goy, 1979. Bown and Cooper in Bown, pl. 4.1, figs. 4–5; pl. 4.9, figs. 6–7.
2006 *Crepidolithus cavus* Prins ex Rood et al., 1973. Perilli and Duarte, pl. 2, fig. 16.
2007 *Crepidolithus cavus* Prins ex Rood et al., 1973. Fraguas et al., pp. 233–236, pl. 1, fig. 2.
2014 *Crepidolithus cantabriensis* Fraguas, pp. 33–36, figs. 3a–e (non fig. f).
2019 *Crepidolithus cavus/impontus* Prins ex Rood et al., 1973. Menini et al., p. 16, pl. 1, fig. 11.

*Range*. Pliensbachian–Bajocian (Bown and Cooper, 1998).

*Occurrence*. This species has been recorded in the entire studied interval.

*Remarks*. *Crepidolithus impontus* was first introduced by Grün et al. (1974, p. 310), who describe "a large coccolith whose central area is spanned in the proximal side by a bridge made up of two rows of elements parallel to the short axis of the ellipse. A central process is absent". Goy (in Goy et al., 1979, p. 39) emended this diagnosis and proposed "A species of the genus *Crepidolithus* with a wall composed of calcite laths very inclined and overlapping. The central area is spanned by a bridge parallel to minor axis of the ellipse having in its centre a very small spine". Grün et al. (1974) stated in their remarks that *C. impontus* resembles to *C. cavus sensu* Prins, 1969 (nomen nudum). The diagnosis by Goy (in Goy et al., 1979) closely resembles that of *C. cavus*, which is a species of *Crepidolithus* with a bridge along the minor axis of the elliptical central area (Rood et al., 1973, p. 375). Accordingly, Bown (1987b) considers *C. impontus* to be a junior synonym of *C. cavus*. Eventually, Bown and Cooper (1998) use *C. cavus* for early Pliensbachian forms with a prominent spine (which according to the description might rather be considered *P. liasicus*) without figuring it and *C. impontus* to refer to late Pliensbachian specimens with a wide central area spanned by a delicate bridge and no spine. The specimen of *C. cavus* drawn by Prins (1969, nomen nudum) figures a murolith with a relatively reduced central area and two prominent insertions of a central structure. The overall features of this specimen may look like a *Parhabdolithus liasicus*. Thus, *C. cavus* informally introduced by Prins (1969) was validated by Rood et al. (1973), who show for the holotype an SEM image having a relatively narrow central area and a prominent spine. Also, because the SEM

image is very poor, sutural lines of the distal shield are not visible and this specimen resembles a *Parhabdolithus*. Grün et al. (1974) came to a similar conclusion, stating that the specimen figured by Rood et al. (1973) looks like a distal view of *Parhabdolithus marthae*. Accordingly, de Kaenel et al. (1996) proposed the new combination *Parhabdolithus cavus* (Prins, 1969 ex Rood et al., 1973). Thereby, *C. cavus* in Prins, 1969 ex Rood et al. (1973) should be considered either *P. cavus* or a junior synonym of *P. liasicus* Deflandre, 1952.

The confusion between *C. cavus* (or *P. liasicus*) and *C. impontus* is partly due to the loss of the bridge of *C. impontus* that can be broken in poorly preserved material, making the central area empty; however, the insertions of the bridge are still visible in the wide central area. Also, a certain variability can be observed in the wideness of the central area. *Crepidolithus cantabriensis* introduced by Fraguas (2014) is pro parte considered to be a *C. impontus* here. In the LM images shown by Fraguas (2014, figs. 3a–e) it is difficult to see the insertions of the bridge because the pictures were not taken at 45°. In her original diagnosis, Fraguas describes *C. cantabriensis* as "A medium-sized, normal to narrowly elliptical species of *Crepidolithus* with an open central area. Its thick proximal shield extends distally to form a collar which appears to be a distal inner cycle. Its bicyclic rim extinction pattern results in a sigmoidal interference figure" (p. 35). However, this diagnosis is invalid because the sigmoidal extinction pattern is the result of the optical discontinuity existing between the proximal and distal shield at 45°, which is also a typical feature of *C. impontus*.

***Crepidolithus pliensbachensis*** (Crux, 1985) emend. Bown, 1987b
(Plate 1, fig. 8)

1984 *Crepidolithus ocellatus* Crux, p. 168, figs. 11.3, 5–6, 14.6–7.
1985 *Crepidolithus pliensbachensis* Crux, p. 31 (nomen nudum).
1987b *Crepidolithus pliensbachensis* (Crux, 1985) emend. Bown, pp. 17–18, pl. 1, figs. 16–18; pl. 2, figs. 1–3; pp. 74–75, pl. 12, figs. 9–10.
1992 *Crepidolithus pliensbachensis* (Crux, 1985) Bown, 1987b. Baldanza and Mattioli, pl. 1, fig. 3.
non 1992. *Crepidolithus pliensbachensis* (Crux, 1985) Bown, 1987b. Cobianchi, p. 104, figs. 22i–l.
1994 *Crepidolithus pliensbachensis* (Crux, 1984) Bown, 1987b. Goy et al., pl. 7, figs. 1–2.
1998 *Crepidolithus pliensbachensis* Crux, 1985. Bown and Cooper in Bown, pl. 4.1, figs. 9–10; pl. 4.9, figs. 11–12.
1999 *Crepidolithus pliensbachensis* (Crux, 1984) Bown, 1987b. Mattioli and Erba, pp. 364–365, pl. 1, fig. 7.
2000 *Crepidolithus pliensbachensis* (Crux, 1984) Bown, 1987b. Walsworth-Bell, p. 51, fig. 4.7; p. 90, fig. 6.3.
2008 *Crepidolithus pliensbachensis* (Crux, 1985) Bown, 1987b. Fraguas et al., pl. 1, fig. 2.
2017 *Crepidolithus pliensbachensis* Crux, 1985. Peti et al., p. 11, fig. 5J.
2019 *Crepidolithus pliensbachensis* Crux, 1985. Ferreira et al., p. 8, pl. 1, fig. 26.

*Range*. Hettangian–Pliensbachian (Bown and Cooper, 1998; Mattioli and Erba, 1999).

*Occurrence*. The presence of this species in the El Matuasto I is very rare and only recorded within the NJT4c subzone (spanning Davoei and the very base of the Margaritatus SAZ in Ferreira et al., 2019), where its LO happens. The LO reported by Bown and Cooper (1998) and Mattioli and Erba (1999) within the *ibex* zone probably corresponds to the LCO registered by Ferreira et al. (2019) in the same ammonite zone of Portugal. *Crepidolithus pliensbachensis* is considered a good marker species in the boreal and Tethys realms for the Early Jurassic (Bown et al., 1988; Bown and Cooper, 1998; Mattioli and Erba, 1999). According to Angelozzi and Pérez Panera (2016), the LO of this species is a useful event in the Neuquén Basin, and it occurs within the *Fanninoceras fannini* NAZ, which is considered the time equivalent of the upper part of the Davoei and Margaritatus SAZs (Riccardi, 2008b). In this study, its presence is scarce but continuous, and hence we consider *C. pliensbachensis* to be an important element to make correlations with other regions.

*Remarks*. A typical *Crepidolithus* with a thick distal rimwall and a reduced, lenticular central area spanned by a small spine, typically bow-tie-shaped, which is very diagnostic in LM.

***Crepidolithus timorensis*** (Kristan-Tollmann, 1988a) Bown in Bown and Cooper, 1998
(Plate 1, fig. 11)

1988a *Timorhabdus timorensis* Kristan–Tollmann, pp. 74–75, pl. 1, fig. 6.; pl. 2, figs. 1–6.
1995 "small" *Crepidolithus*. Lozar, p. 110, pl. 1, fig. 3–4.
1998 *Crepidolithus timorensis* (Kristan-Tollmann, 1988a) Bown in Bown and Cooper, pl. 4.1, figs. 11–12; non pl. 4.9, figs. 13–15.

*Range*. Sinemurian–Pliensbachian (Bown and Cooper, 1998; this study).

*Occurrence*. *Crepidolithus timorensis* is assigned to the Sinemurian of Timor (Bown, 1992; Bown and Cooper, 1998). Here we found it in the early Pliensbachian within the NJT4b subzone, probably corresponding to the LO of this species, as previously reported by Lozar (1995, northern Italy and southern France), Mattioli et al. (2013, Portugal), Peti et al. (2017, northern France), and Ferreira et al. (2019, Portugal). This represents the first record of the species in the Neuquén Basin. Reworking is not considered due to the absence of older marine sediments in the area, even though they are present in the north of the basin (Riccardi et al., 1988,

1991; Legarreta and Uliana, 1996; Riccardi, 2008a; Arregui et al., 2011; Legarreta and Villar, 2012).

*Remarks*. Kristan-Tollmann (1988a, p. XVIV/86) provided the diagnosis of this species: "... broadly elliptical coccolith with high and blocky distal shield. The elements forming the distal shield are elongated and enlarged at their extremity. The central-area size is therefore reduced. The spine is short, ending at or just above the rim. The proximal shield is flat and composed of small elements. In the centre is a weakly developed rhombic structure, made evident by few loose elements (see holotype figs. 3, 5, pl. 2). The elements of the proximal shield are arranged to form two perpendicular furrows, aligned with the major and minor axes of the ellipse. In the case of poorly preserved coccoliths or etched specimens, only the central hole and the cross–shaped furrow can be seen proximally (see plate 2, fig. 1,2,6)". *Crepidolithus timorensis* is observed in this study as a small coccolith (less than 4.5 µm) with an irregular outline due to the large size of the elements forming the distal shield. The small spine often appears as a small cluster of irregular calcite crystals. Lozar (1995; p. 110) identified a "small" *Crepidolithus* described as an "elliptical coccolith very similar to *C. crassus* with a comparable blocky structure, but smaller in size; the elongated central area is closed by a wavy suture". Despite the fact that this description does not match the original diagnosis of *Crepidolithus timorensis*, the pictures provided correspond to the species because the irregular spine can be seen in one of them. The "small" *Crepidolithus* mentioned in Cobianchi (1992, p. 104) or *C. timorensis* pictured by Bown and Cooper (1998) in pl. 4.1, figs. 11–12 should not be confused with the *C. crassus* "small morphotype" introduced by Suchéras-Marx et al. (2010). Conversely, the pictures shown by Bown and Cooper (1998) pl. 4.9, figs. 13–14 as *C. timorensis* are *C. crassus* small morphotypes. In fact, *C. timorensis* differs from the *C. crassus* small morphotype due to its smaller size (4.5 µm vs. 6.5 µm on average), but also because of its irregular outline, which is due to the presence of blocky elements composing the distal shield. Conversely, the outline of small *crassus* is very smooth.

Genus ***Tubirhabdus*** Prins ex Rood et al., 1973

*Type species*. *Tubirhabdus patulus* Prins, 1969 ex Rood et al., 1973

***Tubirhabdus patulus*** Prins, 1969 ex Rood et al., 1973

*Range*. Sinemurian–Tithonian (Bown and Cooper, 1998).

*Occurrence*. *Tubirhabdus patulus* is reported to be a an extremely long-ranging species, and it is observed throughout the studied interval.

*Remarks*. This is a narrowly elliptical coccolith with a central-area structure that supports a broad, hollow spine. Although the holotype dimensions state a coccolith smaller than 4 µm (Rood et al., 1973), the size range of our studied material goes from 2.75 to 7 µm. Three discrete morphotypes of this species were identified in the studied material based upon size and thickness of the rim. Herein, the "thin" and "thick" morphotypes are partly equivalent to the *T. patulus* "small" (pl. 4.9, figs. 16–17, p. 71) and "large" (pl. 4.9, figs. 18–19, p. 71) illustrated by Bown and Cooper (1998). A third morphotype is represented by tiny coccoliths clearly displaying a tube-like spine in the reduced central area. Kristan-Tollmann (1988b) introduced two subspecies mainly based on the spine shape and dimensions, namely *T. patulus patulus* (pl. 3, figs. 2–6; pl. 5, fig. 8) and *T. patulus tubaformis* (pl. 3, figs. 2–4, 7–8). However, the differences in the spine morphology are difficult to observe with LM.

This species is very abundant in the studied section, constituting 22 % of the total coccolith abundance. Moreover, a shift in the proportions occurs from the base to the top of El Matuasto I between thick and thin *T. patulus*. Further analysis is necessary to elucidate if these morphotypes respond to preservation or ecological factors.

***Tubirhabdus patulus*** Prins, 1969 ex Rood et al., 1973 (tiny morphotype)
(Plate 1, fig. 12)

1973 *Tubirhabdus patulus* Prins, 1969 ex Rood et al., pp. 373–374, pl. 2, fig. 3.
1979 *Tubirhabdus patulus* Prins, 1969 ex Rood et al., 1973. Medd, p. 45, pl. 9, fig. 9.
1982 *Tubirhabdus patulus* Prins, 1969 ex Rood et al., 1973. Hamilton in Lord, pl. 3.1, fig. 20.
1987a *Tubirhabdus patulus* Prins, 1969 ex Rood et al., 1973. Bown, pl. 1, figs. 3–4.
1987b *Tubirhabdus patulus* Prins, 1969 ex Rood et al., 1973. Bown, pp. 18–20, pl. 2, figs. 4–6; pl. 12, figs. 11–12.
1988a *Tubirhabdus patulus* Prins, 1969 ex Rood et al., 1973. Kristan–Tollmann, pp. 72–73, pl. 1, fig. 1, 5 (top right).
1988b *Tubirhabdus patulus patulus* Prins, 1969 ex Rood et al., 1973 n. ssp. Kristan–Tollmann, pp. 116–117, pl. 3, figs. 2–6; pl. 5, fig. 8.
1992 *Tubirhabdus patulus* Prins, 1969 ex Rood et al., 1973. Cobianchi, p. 104, fig. 22n.
1998 *Tubirhabdus patulus* Rood et al., 1973. Bown and Cooper in Bown, pl. 4.1, fig. 13.
2013 small *Tubirhabdus patulus* Rood et al., 1973. Mattioli et al., pl. 1, figs. 1.

*Remarks*. This morphotype is represented by small coccoliths with a proportionally bigger spine compared to its overall size. It better applies to the holotype diagnosis by Rood et al. (1973, p. 373): "A small species of *Tubirhabdus* with a very broadly open oval to circular central spine". The holotype dimensions state a coccolith smaller than 4 µm; accordingly, in this contribution the pictures provided for the synonymy list comprise specimens between 2.75 and 4.6 µm.

***Tubirhabdus patulus*** Prins, 1969 ex Rood et al., 1973 (thin morphotype)
(Plate 1, figs. 13–14)

1969 *Tubirhabdus patulus* Prins, pl. 1, fig. 10B–C (non fig. 10A) (nomen nudum).
1974 *Tubirhabdus patulus* Prins, 1969 ex Rood et al., 1973. Barnard and Hay, pl. 1, fig. 4.
1982 *Tubirhabdus patulus* Prins, 1969 ex Rood et al., 1973. Hamilton in Lord, pl. 3.1, fig. 16.
1995 *Tubirhabdus patulus* Prins, 1969 ex Rood et al., 1973. Lozar, p. 110, pl. 1, fig. 10.
1998 *Tubirhabdus patulus* Rood et al., 1973. Bown and Cooper in Bown, pl. 4.1, fig. 14; pl. 4.9, figs. 16–17.
2000 *Tubirhabdus patulus* Prins, 1969 ex Rood et al., 1973. Walsworth-Bell, p. 51, fig. 4.7; p. 90, fig. 6.3.
2008 *Tubirhabdus patulus* Prins, 1969 ex Rood et al., 1973. Aguado et al., fig. 5.35–36.
2017 *Tubirhabdus patulus* Prins, 1969 ex Rood et al., 1973. Peti et al., p. 11, fig. 5Y.
2019 *Tubirhabdus patulus* Rood et al., 1973. Menini et al., pl. 1 (thin).
2021 *Tubirhabdus patulus* Rood et al., 1973. Fraguas et al., fig. 9, CM.255.

*Remarks*. This morphotype comprises specimens with two central-area dimensions: coccoliths with a broadly open, rectangular central area (Prins, 1969, pl. 1 fig. 10C; Bown, 1987b, pl. 12, figs. 11–12) and specimens with a narrowly elliptical, elongated central area (lozenge-like) (Prins, 1969, pl. 1., fig. 10A). Both are spanned by a median structure that supports a thin, sometimes oval spine, like in the drawing of Prins (1969, pl. 1, fig. 10B).

The coccolith dimensions are usually bigger (5–7 µm) than the holotype description, and the specimens in synonymy are comprised between 4.7 and 6.2 µm.

***Tubirhabdus patulus*** Prins, 1969 ex Rood et al., 1973 (thick morphotype)
(Plate 1, figs. 15–16)

1969 *Tubirhabdus patulus* Prins, pl. 1, fig. 10A–B (non fig. 10C) (nomen nudum).
1982 *Tubirhabdus patulus* Prins, 1969 ex Rood et al., 1973. Hamilton in Lord, pl. 3.4, fig. 10.
?1988 *Parhabdolithus leiassicus* Deflandre, 1954. Angelozzi, p. 142, pl. 2, fig. 9.
1998 *Tubirhabdus patulus* Rood et al.,1973. Bown and Cooper in Bown, pl. 4.9, figs. 18–19.
1995 *Tubirhabdus patulus* Prins, 1969 ex Rood et al., 1973. Lozar, p. 110, pl. 1, figs. 11–12.
2006 *Tubirhabdus patulus* Prins, 1969 ex Rood et al., 1973. Perilli and Duarte, pl. 2, fig. 5.
2010 *Tubirhabdus patulus* Rood et al., 1973. Reggiani et al., pl. 1.16.
2019 *Tubirhabdus patulus* Rood et al., 1973. Menini et al., pl. 1 (thick).

*Remarks*. Slightly elliptical coccoliths showing a very reduced oval central area infilled by a thick spine. Medd (1979) already stated that the *T. patulus* proximal view may be confused under the LM with *Mitrolithus elegans* because in both species the base of a hollow spine is visible. However, the proximal shield architecture is different in the two species. The *Tubirhabdus patulus* proximal shield is composed of small elements surrounding a broadly open central area, and the foci of the asymmetrical extinction cross are very far away along the major axis of the ellipsis, while the *M. elegans* proximal shield elements are blocky, making the central opening very reduced, and the foci of the extinction cross are in contact with the base of the hollow spine. Prins (1969) nicely illustrated such features (pl. 1, figs. 10A–11A).

Order STEPHANOLITHIALES Bown and Young, 1997

Family PARHABDOLITHACEAE Bown, 1987b

Genus ***Crucirhabdus*** Prins ex Rood et al., 1973

*Type species*. *Crucirhabdus primulus* Prins, 1969 ex Rood et al., 1973, emend. Bown, 1987b

***Crucirhabdus primulus*** Prins, 1969 ex Rood et al., 1973, emend. Bown, 1987b
(Plate 2, figs. 1–2)

1969 *Crucirhabdus primulus* var. *nanus* Prins, p. 551, pl. 1, fig. 1A–B; pl. 2, fig. 1A–B; pl. 3, fig. 1A–B (nomen nudum).
1969 *Crucirhabdus primulus* var. *primulus* Prins, p. 552, pl. 2, fig. 2A (non fig. 2B); pl. 3, fig. 2A (non fig. 2B) (nomen nudum).
1969 *Crucirhabdus primulus* var. *striatulus* Prins, p. 554, pl. 3, fig. 3A–B (nomen nudum).
1973 *Crucirhabdus primulus* Prins ex Rood et al., pp. 367–368, pl. 1, figs. 1–2.
1979 *Apertius dorei* Goy in Goy et al., p. 40, pl. 2, fig. 6.
1981 *Apertius dorei* Goy, 1979; Goy, pl. 9, figs. 9–10; pl. 10, figs. 1–3; text-fig. 8.
1987b *Crucirhabdus primulus* Prins, 1969 ex Rood et al., 1973 emend. Bown, pp. 23–24, pl. 2, figs. 15–18; pl. 3, figs. 1–3; pl. 12, figs. 17–20; text-fig. 10.
1998 *Crucirhabdus primulus* Rood et al., 1973. Bown and Cooper in Bown, pl. 4.2, figs. 9–11; pl. 4.10, figs. 14–15.
2000 *Crucirhabdus primulus* Rood et al., 1973. Walsworth-Bell, p. 51, fig. 4.7; p. 90, fig. 6.3.
2010 *Crucirhabdus primulus* Rood et al., 1973. Reggiani et al., pl. 1., fig. 2.
2013 *Crucirhabdus primulus* Rood et al., 1973. Mattioli et al., pl. 1, fig. 16.
2019 *Crucirhabdus primulus* Rood et al., 1973. Menini et al., pl. 1.
2019 *Crucirhabdus primulus* Rood et al., 1973. Ferreira et al., pl. 1.

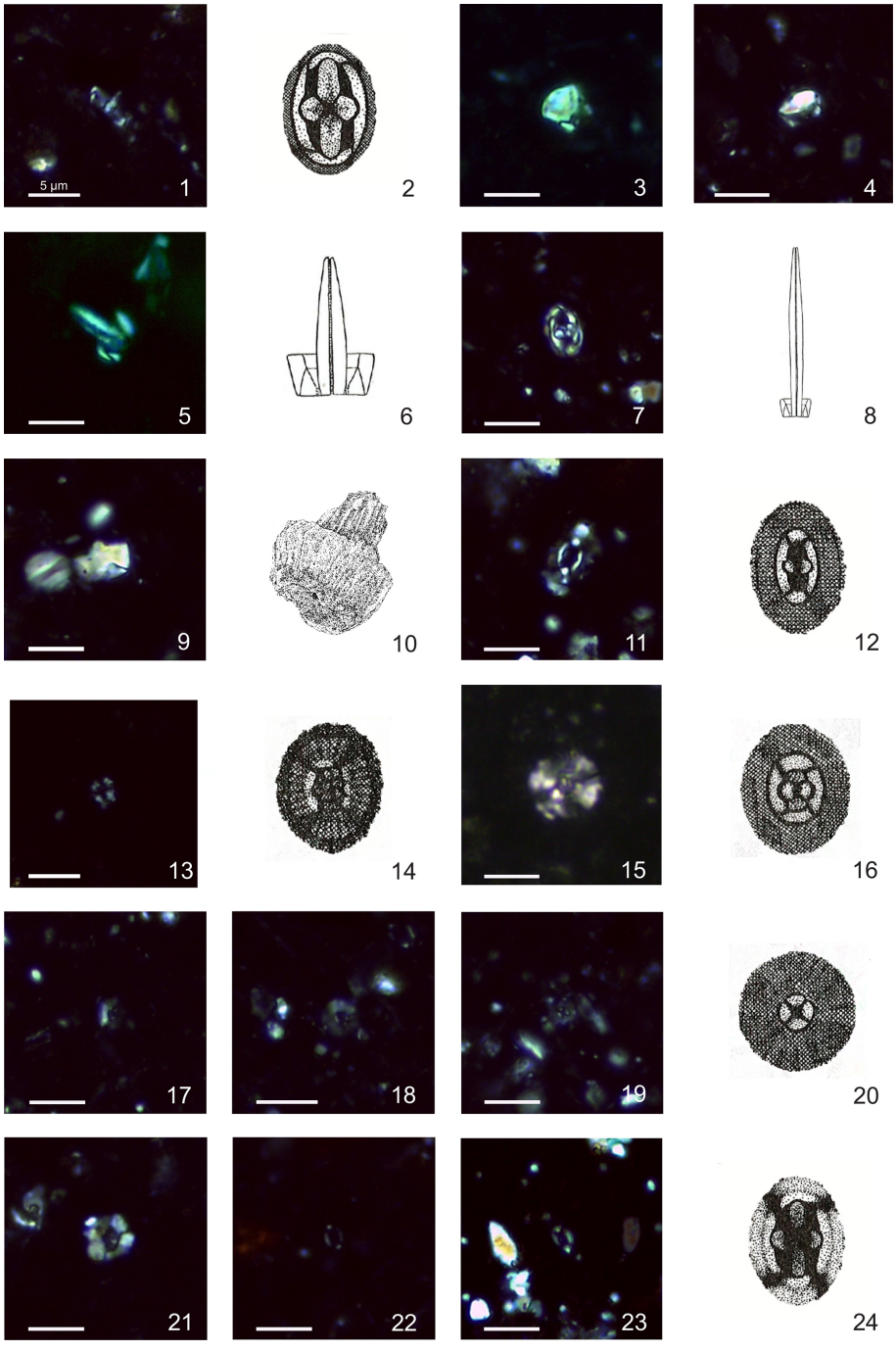


**Plate 2.** Calcareous nannofossils from El Matuasto I, Los Molles Formation, Neuquén Basin. All pictures from LM under crossed nicols and distal view unless specified. Scale bar: 5 µm. Illustrations adapted after Prins (1969) except fig. 10 after Noël (1965b). **(1, 2)** *Crucirhabdus primulus* Prins, 1969 ex Rood et al., 1973 emend. Bown, 1987b, side and distal view, EM-I-19 (YT.RMP_N.000012.11). **(3)** *Mitrolithus elegans* Deflandre, 1954, side view, EM-I-1 (YT.RMP_N.000012.1). **(4)** *Mitrolithus lenticularis* Bown, 1987b, side view, EM-I-13 (YT.RMP_N.000012.6). **(5, 6)** *Parhabdolithus liasicus* spp. *distinctus* (Deflandre, 1952) Bown, 1987b, side view, EM-I-15 (YT.RMP_N.000012.8). **(7, 8)** *Parhabdolithus liasicus* spp. *liasicus* (Deflandre, 1952) Bown, 1987b, distal and side view, EM-I-12 (YT.RMP_N.000012.5). **(9, 10)** *Parhabdolithus robustus* Noël, 1965b, side view, EM-I-18 (YT.RMP_N.000012.10). **(11, 12)** *Biscutum grande* Bown, 1987b, EM-I-16 (YT.RMP_N.000012.9). **(13, 14)** *Similiscutum finchii* (Crux, 1984 emend. Bown, 1987a) de Kaenel and Bergen, 1993, EM-I-23 (YT.RMP_N.000012.13). **(15, 16)** large *Similiscutum* aff. *finchii* (Crux, 1984 emend. Bown, 1987a) de Kaenel and Bergen, 1993, EM-I-26 (YT.RMP_N.000012.16). **(17, 20)** *Similiscutum cruciulus* group, EM-I-18 (YT.RMP_N.000012.10). **(21)** *Calyculus* sp. Noël, 1972, EM-I-16 (YT.RMP_N.000012.9). **(22)** *Lotharingius barozii* Noël, 1972, early morphotype, EM-I-19 (YT.RMP_N.000012.11). **(23, 24)** *Lotharingius barozii* Noël, 1972, typical morphotype, EM-I-23 (YT.RMP_N.000012.13).

*Range*. Norian–Toarcian (Bown and Cooper, 1998).

*Occurrence*. This species is a characteristic north-western Europe component (boreal realm; Bown, 1987b) and tends to be scarce in Tethyan localities during the Early Jurassic (Bown, 1987b; Fraguas et al., 2018). In El Matuasto I, this species was recorded consistently from the base to the top of the section (NJT4a–c zones).

*Remarks*. In the present study *C. primulus* is widely recognized in side view under the LM and differs from *Parhabdolithus liasicus* by having a low rim that gives it a "flat" appearance. The proximal shield appears as two tooth-like elements which are very far away each other because of the presence of a widely open central area. The presence or absence of the spine depends on the preservation quality. Small specimens resembling the variety *C. primulus nanus* described in Prins (1969) were sporadically observed. The recognition of *C. primulus* in distal view could be difficult because the delicate cross-structure may be easily broken.

Genus ***Mitrolithus*** Deflandre in Deflandre and Fert, 1954 emend. Bown and Young in Young et al., 1986

*Type species*. *Mitrolithus elegans* Deflandre in Deflandre and Fert, 1954

***Mitrolithus elegans*** Deflandre, 1954
(Plate 2, fig. 3)

1954 *Mitrolithus elegans* Deflandre in Deflandre and Fert, p. 148, pl. 15, figs. 9–11; text-figs. 66–67.
1965 *Alvearium dorsetense* Black, pp. 133, 136, fig. 5.
1986 *Mitrolithus elegans* Deflandre, 1954. Young et al., pl., figs. I, L.
1987b *Mitrolithus elegans* Deflandre, 1954. Bown, pp. 26–27, pl. 3, figs. 6–15; pl. 12, figs. 23–28.
1988b *Mitrolithus elegans* Deflandre, 1954. Kristan–Tollmann, p. 114, pl. 1, figs. 6–7.
1998 *Mitrolithus elegans* Deflandre, 1954. Bown and Cooper in Bown, pl. 4.2, figs. 13–14; pl. 4.10, figs. 18–20.
2000 *Mitrolithus elegans* Deflandre, 1954. Walsworth-Bell, p. 51, fig. 4.7; p. 90, fig. 6.3.
2008 *Mitrolithus elegans* Deflandre, 1954. Fraguas et al., pl. 1, fig. 4.
2010 *Mitrolithus elegans* Deflandre, 1954. Reggiani et al., pp. 2–3, pl. 1., fig. 13.
2013 *Mitrolithus elegans* Deflandre, 1954. Mattioli et al., pl. 1, fig. 13.
2017 *Mitrolithus elegans* Deflandre, 1954. Peti et al., p. 11, fig. 5F.

*Range*. Hettangian–Pliensbachian (Bown and Cooper, 1998; Mattioli and Erba, 1999).

*Occurrence*. This species is a typical component of Tethys and north-eastern Pacific assemblages (Bown, 1987b, 1992; Bown and Lord, 1990; Ferreira et al., 2019) and is rarely observed in north-western European associations during the lower Sinemurian to the lower Toarcian (Bown 1987b, 1992; Mattioli and Erba, 1999). In the El Matuasto I section, we found the first record of common and consistent occurrence of *M. elegans* in the south-eastern Pacific area in the early Pliensbachian.

*Remarks*. *Mitrolithus* species, and especially *M. elegans*, can be observed in both plan view (proximal or distal) and side view, which is more diagnostic. In this study, *Mitrolithus elegans* was usually observed in side view, having a prominent spine protruding from the distal shield of the coccolith. Specimens observed in proximal view were also common. Isolated spines (corresponding to the *A. dorsetensis* of Black, 1969) were rarely observed. The holotype dimensions are 5.8 µm length and 6 µm height (Deflandre in Deflandre and Fert, 1954). Differences between *M. elegans* and *T. patulus* have been discussed above.

***Mitrolithus lenticularis*** Bown, 1987b
(Plate 2, fig. 4)

1987b *Mitrolithus lenticularis* Bown, pp. 28–30, pl. 4, figs. 4–7; pl. 12, figs. 29–30.
1988b *Mitrolithus lenticularis* Bown, 1987b. Kristan–Tollmann, p. 115, pl. 1, figs. 3–5.
non 1992 *Mitrolithus lenticularis* Bown, 1987b. Cobianchi, fig. 20n.
1998 *Mitrolithus lenticularis* Bown, 1987b. Bown and Cooper in Bown, pl. 4.2, figs. 17–18; pl. 4.10, figs. 24–25.
2010 *Mitrolithus lenticularis* Bown, 1987b. Reggiani et al., pp. 2–3, pl. 1, figs. 14–15.
2013 *Mitrolithus lenticularis* Bown, 1987b. Mattioli et al., pl. 1, fig. 9–10.
? 2015 *Mitrolithus lenticularis* Bown, 1987b. Casellato and Erba, pl. 1.25.
2019 *Mitrolithus lenticularis* Bown, 1987b. Menini et al., pl. 1.

*Range*. Sinemurian–Pliensbachian (Mattioli and Erba, 1999).

*Occurrence*. *M. lenticularis* occurs consistently and abundantly in El Matuasto I from the base of the section, dated as early Pliensbachian (NJT4 biozone). Angelozzi and Pérez Panera (2016) noticed that this species is characteristic of the Pliensbachian–Toarcian boundary assemblages in the Neuquén Basin. Bown (1987b, 1992) and Bown and Cooper (1998) considered *M. lenticularis* a typical Tethyan species. Its presence in the Neuquén Basin is crucial to establish palaeobiogeographic relationships between the south-eastern Pacific and the Tethys realms.

*Remarks*. *Mitrolithus lenticularis*, which is usually recognized in side view, differs from *M. elegans* because of its slightly smaller size (Holotype dimensions are 4.5 µm length, 3.7 µm height; Bown, 1987b) and because it has a lenticular spine that does not protrude from the rim.

Genus ***Parhabdolithus*** Deflandre in Grassé, 1952 emend. Bown, 1987b

*Type species*. *Parhabdolithus liasicus* Deflandre in Grassé, 1952

***Parhabdolithus liasicus*** Deflandre in Grassé, 1952

*Range*. Hettangian–Toarcian (Bown and Cooper, 1998).

*Remarks*. This taxon has a high rim and a transverse bar supporting a spine in the central area. Owing to spine dimorphism, an informal separation within the species was recognized by Prins (1969). Bown (1987b) proposed two subspecies based on previous descriptions and illustrations by Deflandre (1952; in Deflandre and Fert, 1954). *Parhabdolithus liasicus distinctus* has a larger rim and a relatively thick spine compared to *P. liasicus liasicus*, which is a tiny coccolith with an extremely long and thin spine. Both subspecies are consistently present throughout the El Matuasto I section, even though *P. liasicus distinctus* abundance is much higher (88 %) than *P. liasicus liasicus* (12 %).

***Parhabdolithus liasicus distinctus*** (Deflandre, 1952) Bown, 1987b
(Plate 4, figs. 5–6)

1952 *Parhabdolithus liasicus* Deflandre in Grassé, p. 466, text-fig. 362 (J, L, M, non K).
1954 *Parhabdolithus liasicus* Deflandre; Deflandre in Deflandre and Fert, p. 162, text-figs. 105–108 (non 104).
1965b *Parhabdolithus liasicus* Deflandre, 1954. Noël, pl. 3, fig. 7; pl. 4, fig. 7; text-fig. 22a–b, e.
1969 *Parhabdolithus liasicus* Deflandre, 1954. Prins pl. 2, figs. 4A–B.
1969 *Crucirhabdus primulus* var. *primulus* Prins, p. 552, pl. 2, fig. 2B (non fig. 2A); pl. 3, fig. 2B (non fig. 2A) (nomen nudum).
1973 *Parhabdolithus liasicus* Deflandre, 1952. Rood et al., pp. 372–373, pl. 2, fig. 1.
1973 *Crepidolithus cavus* Prins ex Rood et al., p. 375, pl. 2, fig. 5.
1977 *Parhabdolithus liasicus* Deflandre, 1952. Hamilton, pl. 4, fig. 7.
1979 *Parhabdolithus marthae* Deflandre, 1954. Medd, pl. 1, fig. 10.
1982 *Parhabdolithus liasicus* Deflandre, 1952. Hamilton in Lord, pl. 3.1, fig. 5; pl. 3.4, figs. 3–4.
1987b *Parhabdolithus liasicus* Deflandre, 1952. Crux, pl. 1, figs. 14–16; pl. 1, fig. 10.
1987b *Parhabdolithus liasicus distinctus* Deflandre, 1952. Bown, pp. 30–31, pl. 4, figs. 10–15; pl. 13, figs. 5–8.
1992 *Parhabdolithus liasicus* Deflandre, 1954. Baldanza and Mattioli, pl. 1, fig. 9.
1992 *Parhabdolithus liasicus distinctus* (Deflandre, 1952) Bown, 1987b. Cobianchi, p. 98, fig. 21a–b.
1998 *Parhabdolithus liasicus* Deflandre in Grasse, 1952 ssp. *distinctus* Bown, 1987b. Bown and Cooper in Bown, pl. 4.2, figs. 19–20; pl. 4.10, figs. 26–29.
2000 *Parhabdolithus liasicus liasicus* (Deflandre, 1952) Bown, 1987b. Walsworth-Bell, p. 51, fig. 4.7; p. 90, fig. 6.3.
2006 *Parhabdolithus liasicus liasicus* (Deflandre, 1952) Bown, 1987b. Perilli and Duarte, pl. 2, fig. 15.
2008 *Parhabdolithus liasicus distinctus* (Deflandre, 1952) Bown, 1987b. Fraguas et al., pl. 1, fig. 3.
2013 *Parhabdolithus liasicus liasicus* (Deflandre, 1952) Bown, 1987b. Mattioli et al., pl. 1, figs. 3–6, 8.
non 2013 *Parhabdolithus liasicus* Deflandre, 1954. Rai and Jain, pl. 1, fig. 10a–c.
2017 *Parhabdolithus liasicus* Deflandre, 1952. Peti et al., figs. S.1 6-11 (non 7; appendix F).
2019 *Parhabdolithus liasicus distinctus* (Deflandre, 1952) Bown, 1987b. Ferreira et al., pl. 2.

*Remarks*. *Parhabdolithus liasicus distinctus* is usually observed in side view, showing a high rim with a slightly thin, tapering spine that is double the height of the rim. The coccolith length dimensions provided by Bown (1987b, p. 30) are 3.7–6.8 µm and in our specimens range from 4 to 6 µm. They are often strongly overgrown. In distal view, the base of the spine provides an extinction pattern with a clover-like structure aligned with the minor axis of the ellipse.

***Parhabdolithus liasicus liasicus*** (Deflandre, 1952) Bown, 1987b
(Plate 2, figs. 7–8)

1952 *Parhabdolithus liasicus* Deflandre in Grassé, text-fig. 362K.
1954 *Parhabdolithus liasicus* Deflandre in Grassé; Deflandre in Deflandre and Fert, text-fig. 104; pl. 15, figs. 28–31.
1965b *Parhabdolithus liasicus* Deflandre in Grassé, 1952. Noël, pl. 4, figs. 3–4; text-fig. 22c.
1969 *Parhabdolithus longispinus* Prins pl. 2, fig. 5 (nomen nudum).
1987b *Parhabdolithus liasicus liasicus* Deflandre in Grassé, 1952. Bown, p. 31, pl. 4, figs. 16–17; pl. 13, figs. 9–10.
1998 *Parhabdolithus liasicus* Deflandre in Grassé, 1952 ssp. *liasicus*. Bown and Cooper in Bown, pl. 4.3, fig. 1; pl. 4.10, figs. 30–31.
non 2006 *Parhabdolithus liasicus liasicus* (Deflandre, 1952) Bown, 1987b. Perilli and Duarte, pl. 2, fig. 15.
2013 *Parhabdolithus liasicus liasicus* (Deflandre, 1952) Bown, 1987b. Mattioli et al., pl. 1, figs. 7, 11–12.
2017 *Parhabdolithus liasicus* Deflandre, 1952. Peti et al., fig. S.1 7 (appendix F).
2017 *Parhabdolithus liasicus liasicus* (Deflandre, 1952) Bown, 1987b. Peti et al., figs. S.1 12–13 (appendix F).
2019 *Parhabdolithus liasicus liasicus* (Deflandre, 1952) Bown, 1987b. Ferreira et al., pl. 2.

*Remarks*. In this latter morphotype, the rim dimensions are very small, while the spine is thin and very long; the spine is often broken. Dimensions given by Bown (1987b) are 2.8–3.6 µm length and 1.6–2 µm width. The extinction pattern of the spine in plan view forms a central cross showing a butterfly-like structure aligned with the minor axis of the ellipse.

***Parhabdolithus robustus*** Noël, 1965b
(Plate 2, figs. 9–10)

1965b *Parhabdolithus robustus* Noël, pp. 95–96, pl. 4, figs. 1–2, text-fig. 24.
1987b *Parhabdolithus zweilii* Crux, p. 95; pl. 1, figs. 1–4.
1987a *Parhabdolithus robustus* Noël, 1965b. Bown, p. 43, pl. 1, figs. 5–6; pl. 2, figs. 8–9.
1987b *Parhabdolithus robustus* Noël, 1965b. Bown, p. 34, pl. 5, figs. 3–6; pl. 13, figs. 15–16.
1992 *Mitrolithus lenticularis* Bown, 1987b. Cobianchi, p. 98, fig. 20n.
1998 *Parhabdolithus robustus* Noël, 1965b. Bown and Cooper in Bown, pl. 4.3, figs. 3–4; pl. 4.11, fig. 3.
2013 *Parhabdolithus robustus* Noël, 1965b. Mattioli et al., pl. 1., fig. 2.
2017 *Parhabdolithus robustus* Noël, 1965b. Peti et al., p. 11, fig. 5C.
2019 *Parhabdolithus robustus* Noël, 1965b. Ferreira et al., p. 8, pl. 2.

*Range*. Sinemurian–Pliensbachian (Bown and Cooper, 1998; Mattioli and Erba, 1999; Ferreira et al., 2019).

*Occurrence*. *Parhabdolithus robustus* was herein recorded for the first time in the south-eastern Pacific, with a consistent and relatively abundant occurrence from the early to late Pliensbachian (NJT4 a to c subzones). The species is common in the Early Jurassic assemblages from Tethys and boreal realms (Bown, 1987a, b, 1992; Bown and Cooper, 1998), especially abundant in Timor (Bown, 1987b) and rare in the north-eastern Pacific during the Pliensbachian (Bown, 1992). The different relative abundance of this species in the north-eastern and south-eastern Pacific would suggest a possible ecological factor. The LO of *P. robustus* is recorded in the early Pliensbachian within the NJT4a subzone (Bown and Cooper, 1998; Mattioli and Erba, 1999), while in Argentina its presence is observed at least until the NJT4c subzone according to the zonation of Ferreira et al. (2019).

*Remarks*. This coccolith is mainly observed in side view. It possesses a thick, high rim, which gives it a distinctive blocky appearance and a short, broad spine ending at or just above the rim.

Order PODORHABDALES Rood et al., 1971 emend. Bown, 1987b

Family BISCUTACEAE Black, 1971

Genus ***Biscutum*** Black in Black and Barnes, 1959

*Type species*. *Biscutum testudinarium* Black in Black and Barnes, 1959

***Biscutum grande*** Bown, 1987b
(Plate 2, figs. 11–12)

1969 *Palaeopontosphaera binodosa* Prins, pl. 2, fig. 12 (nomen nudum).
1987b *Biscutum grandis* Bown, pp. 44–45, pl. 6, figs. 4–6; pl. 13, figs. 23–25; text-fig. 11.
1998 *Biscutum grande* Bown, 1987b. Bown and Cooper in Bown, pl. 4.4, fig. 14; pl. 4.12, figs. 15–16.
2004 *Biscutum grande* Bown, 1987b. Mattioli et al., fig. 4E.
2006 *Biscutum grande* Bown, 1987b. Perilli and Duarte, pl. 1., figs. 3–4.
2007a *Biscutum grande* Bown, 1987b. Veiga de Oliveira et al., fig. 5D.
2007b *Biscutum grande* Bown, 1987b. Veiga de Oliveira et al., fig. 1.
2008 *Biscutum grande* Bown, 1987b. Fraguas et al., pl. 1, fig. 9.
2010 *Biscutum grande* Bown, 1987b. Reggiani et al., pp. 6–7, pl. 2., figs. 27–28.
2016 *Biscutum grande* Bown, 1987b. Rai et al., fig. 3.14a–b.
2017 *Biscutum grande* Bown, 1987b. Peti et al., figs. S.3 5–8 (appendix F).
2019 *Biscutum grande* Bown, 1987b. Menini et al., pl. 2. (SN3.57 and LAL18)
2019 *Biscutum grande* Bown, 1987b. Ferreira et al., pl. 1 (Peniche97 and Peniche102.1).

*Range*. Pliensbachian–Toarcian (Bown and Cooper, 1998).

*Occurrence*. The consistent presence of this taxon throughout our section and its biostratigraphic reliability allow an accurate age for the sedimentary succession. The FO defines the base of the NJ5 zone (Bown, 1992) and NJ5b (Bown and Cooper, 1998) and NJT4b subzones (Mattioli and Erba, 1999; Ferreira et al., 2019), correlating with the Ibex–Davoei SAZ boundary. *Biscutum grande* is a species with Tethyan affinities according to Bown (1987b, 1992). Its abundance in the studied samples provide evidence of biogeographic similarities between the south-eastern Pacific and Tethyan assemblages.

*Remarks*. *Biscutum grande* is a large, broadly elliptical coccolith composed of a distal shield formed by radial elements and bearing an inner tube cycle. The central area is large, vacant, and sometimes spanned by a thin bar (Bown, 1987b). Under LM, the distal and proximal shields look dark grey, while the inner tube cycle appears as a conspicuously bright rim surrounding the wide central area (Mattioli et al., 2013). The delicate bar is aligned with the minor axis of the elliptic central area, but frequently it is missing; its insertions in the inner tube cycle are, however, seen as two bright lobes. In some cases, the central area can be filled

with small calcite crystals (Menini et al., 2019; pl. 2, LAL18) or (very rarely) spanned by a cross (Ferreira et al., 2019; pl. 1, Peniche97). According to de Kaenel and Bergen (1993) *Palaeopontosphaera binodosa* Prins, 1969, is a synonym of *Similiscutum finchii*; herein we consider *P. binodosa* to be a synonym of *B. grande*.

Genus ***Similiscutum*** de Kaenel and Bergen, 1993

*Type species*. *Similiscutum cruciulus* de Kaenel and Bergen, 1993

***Similiscutum cruciulus*** de Kaenel and Bergen, 1993 **group** Mattioli et al. 2004
(Plate 2, figs. 17–20)

1969 *Palaeopontosphaera repleta* Prins, pl. 2, fig. 11 (nomen nudum).
1977 *Calyculus cribrum* (Noël 1972) Hamilton, p. 586, pl. 1, fig. 9.
1986 *Biscutum* sp. Young et al., p. 124, plate, fig. F.
1987b *Biscutum dubium* (Noël 1965) Grün in Grün et al. 1974, Crux, p. 89, pl. 2, figs. 4–7.
1990 *Biscutum novum* (Goy 1979) Bown 1987a, Cobianchi, p. 134, fig. 4b.
1990 *Biscutum* aff. *novum* (Goy 1979) Bown 1987a, Cobianchi, p. 134 and 136, fig. 4c.
1992 *Biscutum novum* (Goy 1979) Bown 1987a, Cobianchi (partim) pp. 92–93, fig. 19b (non fig. 19c, d).
1992 *Biscutum* aff. *B. novum* (Goy 1979) Bown 1987a, Cobianchi (partim) p. 93, fig. 19e (non fig. 118).
1993 *Similiscutum avitum* de Kaenel and Bergen, pp. 874–875, pl. 1, figs. 12–14; pl. 2, figs. 1–4.
1993 *Similiscutum cruciulus* de Kaenel and Bergen, pp. 875–876, pl. 2, figs. 5–11.
1993 *Similiscutum orbiculus* de Kaenel and Bergen, pp. 873–874, pl. 1, figs. 1–11.
1998 *Similiscutum cruciulus* de Kaenel and Bergen. Bown and Cooper in Bown, pl. 4.5, figs. 3–4; pl. 4.12, figs. 28–30.
2000 *Similiscutum cruciulus* de Kaenel and Bergen, 1993. Walsworth-Bell, p. 51, fig. 4.7.
2004 *Similiscutum avitum* de Kaenel and Bergen, 1993. Mattioli et al., p. 9, fig. 4b.
2004 *Similiscutum cruciulus* de Kaenel and Bergen, 1993. Mattioli et al., p. 9, fig. 4a.
2004 *Similiscutum orbiculus* de Kaenel and Bergen, 1993. Mattioli et al., p. 9, fig. 4c.
2006 *Similiscutum cruciulus* de Kaenel and Bergen, 1993. Perilli and Duarte, pl. 2, fig. 1.
2006 *Similiscutum cruciulus* de Kaenel and Bergen, 1993. Perilli and Duarte, pl. 2, fig. 2
2007a *Similiscutum cruciulus* de Kaenel and Bergen, 1993. Veiga de Oliveira et al., fig. 6O.
2007a *Similiscutum orbiculus* de Kaenel and Bergen, 1993. Veiga de Oliveira et al., fig. 6N.
2007b *Similiscutum orbiculus* de Kaenel and Bergen, 1993. Veiga de Oliveira et al., fig. 2.
2007b *Similiscutum cruciulus* de Kaenel and Bergen, 1993. Veiga de Oliveira et al., fig. 2.
2010 *Similiscutum cruciulus* de Kaenel and Bergen, 1993. Reggiani et al., pp. 6–7, pl. 2, figs. 29–30.
2019 *Similiscutum orbiculus* de Kaenel and Bergen, 1993. Menini et al., p. 17, pl. 2 (*S. cruciulus orbiculus*).
2021 *Similiscutum avitum* de Kaenel and Bergen, 1993. Fraguas et al., fig. 9, CM.235.1.

*Range*. Pliensbachian–Toarcian (de Kaenel and Bergen, 1993; Bown and Cooper, 1998; Mattioli and Erba, 1999).

*Occurrence*. The presence of the group in this section constitutes the first record in the Early Jurassic for the Neuquén Basin and the second for the south-eastern Pacific Ocean (Fantasia et al., 2018). *Similiscutum cruciulus* is commonly used to define the base of the NJT4 biozone (Bown and Cooper, 1998; Mattioli and Erba, 1999). Due to the clustering criteria and the similar stratigraphic interval (Mattioli et al., 2004), the FO of the *S. cruciulus* group is proposed to define the base of the NJT4 biozone (Ferreira et al., 2019) within the early Pliensbachian and corresponding to the *Jamesoni* SAZ.

*Remarks*. This group includes *S. orbiculus*, *S. avitum*, and *S. cruciulus* (i.e. small, normal to slightly elliptical coccoliths, with a homogeneously grey unicyclic distal shield and a light grey "collar" surrounding the central area). The three species introduced by de Kaenel and Bergen (1993) are roughly differentiated because *S. avitum* shows a broadly elliptical coccolith, *S. orbiculus* has a subcircular outline, and both have a vacant reduced central area, while *S. cruciulus* shows a subcircular outline with a cross spanning the central area. Nevertheless, Mattioli et al. (2004) proposed a clustering for the *Similiscutum cruciulus* group based on the absence of diagnostic biometric differences between the species, highlighting the morphological plasticity within the genus *Similiscutum*.

***Similiscutum finchii*** (Crux, 1984 emend. Bown, 1987a) de Kaenel and Bergen, 1993
(Plate 2, figs. 13–14)

1969 *Striatococcus grandiculus* Prins, pl. 2, fig. 14 (nomen nudum).
non 1969 *Palaeopontosphaera binodosa* Prins, pl. 2, fig. 12 (nomen nudum).
1984 *Biscutum finchii* Crux, p. 168, fig. 9 (3, 4), fig. 13.5.
1987a *Biscutum finchii* Crux, 1984 emend. Bown, p. 44, pl. 2, figs. 3–4, 10–11.
1987b *Biscutum novum* (Goy 1979) Bown 1987a. Bown, p. 77, pl. 13, figs. 19–20.
1987b *Biscutum finchii* Crux, 1984 emend. Bown, 1987a. Bown (partim), pp. 42–44, pl. 5, fig. 18; pl. 6, figs. 1–3; (non pl. 13, figs. 21–22); text-fig. 11.
1992 *Biscutum finchii* Crux, 1984 emend. Bown, 1987a. Baldanza and Mattioli, pl. 1, fig. 12.

1992 *Biscutum finchii* Crux, 1984 emend. Bown, 1987a. Cobianchi, p. 92, fig. 19f–g; text-fig. 18.
1992 *Biscutum* aff. *B. finchii* Crux, 1984 emend. Bown, 1987a. Cobianchi, p. 92, fig. 19i; text-fig. 18.
1992 *Biscutum finchii* Crux, 1984 emend. Bown, 1987a. Reale et al., pl. 1, figs. 5–6.
1993 *Similiscutum finchii* (Crux, 1984 emend. Bown, 1987a) de Kaenel and Bergen, pp. 877–878, pl. 3, figs. 11–13.
1997 *Biscutum finchii* Crux, 1984. Picotti and Cobianchi, pl. 2, fig. 1.
1998 *Biscutum finchii* Crux, 1984. Bown and Cooper in Bown, pl. 4.4, fig. 13; pl. 4.12, figs. 11–14.
non 1998 *Biscutum finchii* (Crux, 1984) Bown, 1987a. Parisi et al., pl. 4, fig. 7
1999 *Biscutum finchii* (Crux, 1984) Bown, 1987a. Mattioli and Erba, p. 365, pl. 1, figs. 19–20.
2002 *Biscutum finchii* Crux, 1984. Perilli and Comas-Rengifo, pl. 1, fig. 13.
2004 *Similiscutum finchii* (Crux, 1984 emend. Bown, 1987a) de Kaenel and Bergen, 1993. Mattioli et al., p. 25, fig. 4j.
2006 *Similiscutum finchii* (Crux, 1984 emend. Bown, 1987a) de Kaenel and Bergen, 1993. Mailliot, pl. 2, figs. 1–4.
2006 *Similiscutum finchii* (Crux, 1984 emend. Bown, 1987a) de Kaenel and Bergen, 1993. Mailliot et al., pl. 1.
non 2006 *Biscutum finchii* (Crux, 1984) Bown, 1987a. Perilli and Duarte, pl. 1, figs. 7–8.
2006 *Biscutum novum* (Goy 1979) Bown, 1987. Perilli and Duarte, pl. 2, figs. 17.
2007a *Biscutum finchii* (Crux, 1984) Bown, 1987a. Veiga de Oliveira et al., fig. 5E–F.
2007b *Biscutum finchii* (Crux, 1984) Bown, 1987a. Veiga de Oliveira et al., fig. 1.
non 2008 *Biscutum finchii* (Crux, 1984) Bown, 1987b. Fraguas et al., pl. 1, fig. 10.
non 2013 *Biscutum finchii* (Crux, 1984) Bown, 1987b. Rai and Jain, pl. 1, figs. 2a–d; pl. 3, figs. 1a–b.
2019 *Similiscutum finchii* (Crux, 1984) Mattioli et al., 2004. Menini et al., p. 17, pl. 2 (SN2.20, LAL18).
2019 *Similiscutum finchii* (Crux, 1984) Mattioli et al., 2004. Ferreira et al., pl. 2 (Peniche12).
2021 *Biscutum finchii* (Crux, 1984) Bown, 1987a. Fraguas et al., fig. 9, CM.235.2.

*Range*. Pliensbachian–Toarcian (Bown and Cooper, 1998).

*Occurrence*. The presence of *S. finchii* in the studied section is observed within the NJT4c subzone. Mattioli et al. (2013) indicate that the FO of this species marks the boundary between the NJ4a and NJ4b subzones within the *Margaritatus* SAZ. This event matches the record of Angelozzi and Pérez Panera (2016) within the equivalent *Fanninoceras fannini* NAZ. According to Riccardi (2008b) the *F. fannini* NAZ correlates with the upper part of the Davoei and most of the Margaritatus SAZ of the western Tethys. In Ferreira et al. (2019), the FO of *S. finchii* occurs simultaneously with the FO of *Lotharingius barozii*, and this latter event marks the base of the NJT4c subzone within the Davoei SAZ (late Pliensbachian) in Portugal. Thus, the record of the FO of *Similiscutum finchii* seems to be quite consistent between Argentina and Portugal.

*Remarks*. Under the LM, *Similiscutum finchii* appears as a medium-sized, normal to broadly elliptical coccolith. The distal shield is light grey with an irregular outline. The central area is narrow, elongated, and sub-rectangular in shape. In SEM pictures (like the holotype), the central area is ogive-shaped, elongated, and narrowly elliptical. Biometrics of *S. finchii* (on average 4.53 µm for the major axis and 3.76 µm for the minor axis; Mattioli et al., 2004) fall at the small end of the range of sizes reported in the literature (Crux, 1984: 5.4–6.6 µm; Bown, 1987b: 5.8–8.5 µm). Morphologically and biometrically, *S. finchii* is quite similar to *S. novum* (average 4.13 µm for the major axis and 3.48 µm for the minor axis; Mattioli et al., 2004), which is, however, overall smaller in size, less elliptical, and with a less developed central area. In the literature, specimens are figured which are larger, more broadly elliptical, and with a more reduced length of the central area than the *S. finchii* holotype description. Such specimens are described here as large *Similiscutum* aff. *finchii* and were designated as *S. giganteum* in Ferreira et al. (2019). De Kaenel and Bergen (1993) considered *Palaeopontosphaera binodosa* Prins, 1969, to be a synonym of *S. finchii*, but we consider *P. binodosa* to be a synonym of *Biscutum grande*. In fact, the drawing in pl. 2, fig. 12 of Prins (1969) shows the presence of a widely open central area spanned by a bridge whose insertions are clearly visible in the inner rim of the coccolith.

**Large *Similiscutum* aff. *finchii*** (Crux, 1984 emend. Bown, 1987a) de Kaenel and Bergen, 1993
(Plate 2, figs. 15–16)

1969 *Palaeopontosphaera crucifera* Prins, pl. 2, fig. 10 (nomen nudum).
1969 *Palaeopontosphaera veterna* Prins, pl. 2, fig. 9 (nomen nudum).
1987b *Biscutum finchii* Crux, 1984 emend. Bown, 1987a. Bown (partim), pl. 13, figs. 21–22).
1998 *Biscutum finchii* (Crux, 1984 emend. Bown, 1987a) de Kaenel and Bergen, 1993. Bown and Cooper, pl. 4.12, figs. 13–14 (large morphotype).
2002 *Biscutum finchii* (Crux, 1984 emend. Bown, 1987a) de Kaenel and Bergen, 1993. Perilli and Comas–Rengifo, pl. 1, fig. 12.
2006 *Similiscutum giganteum* Mailliot, p. 234, pl. 1, figs. 1–6. (nomen nudum)
2006 *Biscutum finchii* (Crux, 1984) Bown, 1987b. Perilli and Duarte, pl. 1, figs. 7–8.

2008 *Biscutum finchii* (Crux, 1984) Bown, 1987b. Fraguas et al., pl. 1, fig. 10.
2014 *Similiscutum giganteum* Mailliot, 2006. Reolid et al., fig. 6. (nomen nudum)
2016 *Similiscutum giganteum* Mailliot, 2006. Da Rocha et al., fig. 7.9–10. (nomen nudum)
2019 *Similiscutum* aff. *S. finchii* (Crux, 1984 emend. Bown, 1987a) de Kaenel and Bergen, 1993. Menini et al., pl. 2 (large, SN3.57B)
2019 *Similiscutum finchii* (Crux, 1984 emend. Bown, 1987a) de Kaenel and Bergen, 1993. Ferreira et al., fig. 2. (nomen nudum).

*Range*. Late Pliensbachian–late Toarcian (Bown, 1987b; Mailliot, 2006; Ferreira et al., 2019).

*Occurrence*. This taxon occurs within the NJT4c subzone in El Matuasto I. It was firstly identified in Argentina by Bown (1987b) as large specimens of *S. finchii*. Mailliot (2006) defines the base of the biostratigraphic range for this taxon in the late Pliensbachian (Margaritatus?–Emaciatum–Spinatum SAZ) in the Peniche section, Lusitanian Basin, Portugal. Ferreira et al. (2019) observed its FO within the NJT4d (Margaritatus SAZ) in the same locality. The occurrence in the studied section would match the previous record in the area (Bown, 1987b) from the late Pliensbachian to the Toarcian.

*Remarks*. This morphotype of *Similiscutum* corresponds to a large, broadly elliptical coccolith with a lozenge–like, reduced central area filled by a robust cross. In the literature, it is typically referred to as large *Similiscutum/Biscutum finchii* (Bown, 1987b; de Kaenel and Bergen, 1993; Bown and Cooper, 1998). Mailliot (2006; unpublished PhD thesis) provided an original diagnosis and proposed *Similiscutum giganteum* as a new and different species from *S. finchii* based on biometric significant differences. However, the introduction of a new species in a PhD thesis is invalid because it does not constitute an effective publication (ICBN, Article 30.9; Turland et al., 2018). We agree with the diagnostic description by Mailliot (2006). Nevertheless, we consider the prompt publication of this species respecting the nomenclature code to be an indispensable and valuable contribution.

Family CALYCULACEAE Noël, 1972

Genus ***Calyculus*** Noël, 1972

*Type species*. *Calyculus cribrum* Noël, 1972

***Calyculus*** sp. indet. Noël, 1972
(Plate 2, fig. 21)

1972 *Calyculus cribum* Noël, p. 116, pl. XII, figs. 1–5.
1979 *Proculithus fistulatus* Medd, p. 54, pl. 10, figs. 8–9.
1979 *Proculithus charlotteii* Medd, p. 55, pl. 10, fig. 11; pl. 11, fig. 9.
1979 *Proculithus expansus* Medd, p. 56, pl. 11, figs. 1, 5–6.
1979 *Incerniculum absolutum* Goy in Goy et al., p. 42, pl. 4, fig. 6.
1979 *Vikosphaera noelae* Goy in Goy et al., p. 42, pl. 4, fig. 7; pl. 5, fig. 1.
1979 *Catillus hommerili* Goy in Goy et al., p. 43, pl. 5, fig. 4.
1979 *Calyculus adjunctus* Goy in Goy et al., p. 42, pl. 5, fig. 2.
1979 *Calyculus cribrum* Noël, 1972; emend. Goy in Goy et al., p. 43, pl. 5, fig. 3.
1987a *Calyculus* sp. Noël, 1972 emend. Crux, p. 53, pl. 1, figs. 13–16.
1987a *Calyculus cribrum* Noël, 1972. Crux, p. 53, pl. 1, figs. 5–7.
1987a *Calyculus* sp. Noël, 1972. Bown, pl. 3, figs. 5–6.
1987b *Calyculus* sp. indet. Noël, 1972. Bown, p. 54, pl. 7, figs. 14–18; pl. 14, figs. 13–14.
1987b *Calyculus cribrum* Noël, 1972 emend. Goy, 1979. Bown, p. 54, pl. 7, fig. 13; text-fig. 15.
1987b *Calyculus depressus* Bown, p. 55, pl. 7, figs. 11–12; text-fig. 15.
1992 *Calyculus cribrum* Noël, 1972 emend. Goy, 1979. Baldanza and Mattioli, pl. 1, fig. 2.
1992 *Calyculus* spp. Noël 1972. Reale et al., pl. 1, figs. 11–14.
1994 *Calyculus* spp. Noël 1972. Goy et al., pl. 7, fig. 8.
1998 *Calyculus* spp. Noël, 1972 indet. Bown and Cooper in Bown, pl. 4.5, fig. 9; pl. 4.13, figs. 2–5.
2006 *Calyculus* spp. Noël 1972. Perilli and Duarte, pl. 2, fig. 4, 18.
2013 *Calyculus* sp. indet. Noël, 1972. Mattioli et al., pl. 2.9–10.
2016 *Calyculus* spp. Noël, 1972. Da Rocha et al., fig. 7.19–20.
2019 *Calyculus* spp. Noël, 1972. Menini et al., pl. 1.
2019 *Calyculus* spp. Noël, 1972. Ferreira et al., pl. 1.
non 2021 *Calyculus* sp. Noël, 1972. Fraguas et al., fig. 9, CM.235.2.

*Range*. Pliensbachian–Bajocian (Bown and Cooper, 1998).

*Occurrence*. The presence of the genus *Calyculus* is recorded in El Matuasto I since the upper part of the lower Pliensbachian section. This changes the previous record in the Neuquén Basin given by Pérez Panera and Angelozzi (2015) and Angelozzi and Pérez Panera (2016) in the early Toarcian within the Tenuicostatum NAZ. Mattioli (1996) and Mattioli and Erba (1999) reported the FO of this taxon in the late Pliensbachian. Bown and Cooper (1998) identified it sporadically in the *ibex* SAZ (early Pliensbachian) and continuously from the *spinatum* SAZ (late Pliensbachian). Afterwards, two morphotypes, namely "small/thin" and "large" *Calyculus*, were reported from the early and late Pliensbachian, respectively (Matti-

oli et al., 2013; Ferreira et al., 2019). The earliest record in El Matuasto I section corresponds to the large morphotype.

*Remarks*. The original diagnosis of the genus *Calyculus* given by Noël (1972, p. 115) describes it as "Elliptical to subcircular coccoliths made up of subvertical elements placed side by side, enlarged and flattened in their distal region; the central area is slightly conical, deep and closed by a grill". Crux (1987a, p. 53) emended it and states that "…Differences in the character of the central grill allow different species to be recognized within the genus *Calyculus*". Bown (1987b) illustrates as "*Calyculus* sp. indet." those specimens which lack central structures and therefore cannot be identified at the species level. We follow the same criterion for our material due to the difficult identification of the grid under LM. However, the literature points out two different groups based on the general shape of the coccolith: big, broadly elliptical specimens (i.e. *Calyculus cribrum*, *C. noeliae*, *C. hommerili*, *C. serrai*, *C. derivatus*, and *C. magnus*) and thin, narrowly elliptical coccoliths (i.e. *Calyculus depressus* and *C. absolutus*). We recognized two morphotypes of this taxon in distal view. One is characterized by a large, thick, and broadly elliptical rim formed by big, trapezoidal elements individually distinguished, giving an irregular outline and an open central area without visible structure. The other morphotype has a slim, narrowly elliptical rim compared to the size of the central area and lacks central structure. Both are very rarely observed in side view.

Order WATZNAUERIALES Bown, 1987b

Family WATZNAUERICEAE Rood et al., 1971

Genus ***Lotharingius*** Noël, 1972 emend. Goy in Goy et al., 1979

*Type species*. *Lotharingius barozii* Noël, 1972 emend. Goy in Goy et al., 1979

Noël (1972, p. 114) described the genus *Lotharingius* as "coccoliths with a rim typical of Lotharingiaceae and the central area with four buttresses aligned with the major and minor axis of the ellipse… additional bars can be also present…".

*Emended diagnosis* (this paper). A placolith–coccolith rim with a bycicilc distal shield. The inner cycle is composed of small elements with radial sutural lines. The outer cycle is composed of elements slightly overlapping and with oblique sutural lines. The central area can be spanned by a cross with additional lateral bars (like *L. barozii*, *L. sigillatus*, *L. crucicentralis*, or *L. umbriensis*), a prominent transversal bar (like in *L. frodoi*), a button (like in *L. hauffi*), or a granular plate (like in *L. velatus*).

*Remarks*. Bown (1987b) considers the cross-structure and lateral bars spanning the central area of *Lotharingius* to be useful distinctive features to differentiate this genus from *Watznaueria*. Mattioli (1996) illustrates the central-area structure variability within the genus and states that a similar cross-structure can be present in the genus *Watznaueria.* Furthermore, Mattioli (1996) points out the arrangement of the shield as the main difference between these two genera. She provides a clear description, stating that *Watznaueria* displays distal shield elements possessing more inclined sutural lines than *Lotharingius* and a prominent concave–convex coccolith shape; under LM "these features produce an extinction pattern with isogyres displaying right angle bent arms, revealing also the net optical discontinuity between the outer and inner cycles of the distal shield. In the genus *Lotharingius* the optical discontinuity in distal view is less marked" (p. 402).

***Lotharingius barozii*** Noël, 1972 emend. Goy in Goy et al., 1979
(Plate 2, figs. 22–24)

1969 *Lucidiella* in*termedia* Prins, pl. 3, fig. 9 (nomen nudum).
1972 *Lotharingius barozi* Noël, pp. 114–115, pl. 11, figs. 1–7; text-fig. 9.
? 1973 *Striatomarginis primitivus* Rood et al., pp. 379–380, pl. 3, fig. 4.
1974 *Lotharingius barozii* Noël, 1972. Grün et al., pp. 303–304, pl. 17, figs. 1–2; text-fig. 7.
1979 *Lotharingius barozi* Noël, 1972 emend. Goy in Goy et al., p. 43, pl. 5, fig. 5.
1981 *Lotharingius barozi* Noël, 1972; Goy, pp. 64–65, pl. 28, figs. 1–9; pl. 29, figs. 1–4.
1984 *Lotharingius crucicentralis* (Medd, 1971); Crux, p. 176, fig. 12 (5).
1987b *Lotharingius barozii* Noël, 1972 emend. Goy in Goy et al., 1979. Bown, p. 70, pl. 10, figs. 7–10; pl. 15, figs. 4–5; text-fig. 17.
1988 *Lotharingius barozii* Noël, 1972. Angelozzi, p. 143, pl. 1, fig. 2.
1994 *Lotharingius barozii* Noël, 1972. Gardin and Manivit, pl. 5, figs. 7–8.
1998 *Lotharingius barozii* Noël, 1972. Bown and Cooper in Bown, pl. 4.7, fig. 15; pl. 4.15, fig. 11.
1999 *Lotharingius barozii* Noël, 1972. Mattioli and Erba, p. 367, pl. 2, fig. 3.
2007 *Lotharingius barozii* Noël, 1972 emend. Goy in Goy et al., 1979. Fraguas et al., pl. 2, fig. 12.
2008 *Lotharingius barozii* Noël, 1972 emend. Goy in Goy et al., 1979. Fraguas et al., pl. 1, fig. 11.
2010 *Lotharingius barozii* Noël, 1972. Reggiani et al., pp. 6–7, pl. 2, fig. 22.
2015 *Lotharingius barozii* Noël, 1972 emend. Goy in Goy et al., 1979. Fraguas et al., fig. 4.6.
2017 *Lotharingius barozii* Noël, 1972. Peti et al., fig. 5S; figs. S.3 34–35 (appendix F).
2017 *Lotharingius barozii* Noël, 1972 emend. Goy in Goy et al., 1979. Ferreira et al., fig. 10.

2019 *Lotharingius barozii* Noël, 1972. Menini et al., p. 17, pl. 2.
2019 *Lotharingius barozii* Noël, 1972. Ferreira et al., pl. 1.

According to the holotype SEM images shown by Noël (1972; pl. 11, fig. 3), neither the original diagnosis "as for the genus (see *Lotharingius* Noël, 1972)" nor the emended diagnosis (Goy, 1979, p. 43) fit the holotype description: "species of the genus *Lotharingius* with a massive buttress aligned with mayor and minor axis of the ellipse and a system of dissymmetric radial bars. The coccosphere is slightly ovoidal and possesses 20 coccoliths".

*Emended diagnosis* (this paper). A placolith–coccolith with a bicyclic distal shield. The inner cycle is composed of small elements with radial sutures. The outer cycle is composed of elements slightly overlapping and with oblique sutural lines. The inner and outer cycles have comparable thickness. The central area is wide and oval and is infilled by buttresses aligned with the major and minor axis of the ellipsis. A few additional lateral bars are visible. In LM images (Bown, 1987b), the coccolith rim is composed of two thin equidimensional cycles surrounding a very wide and elliptical central area spanned by a cross-structure. This delicate structure can be lacking in poorly preserved specimens, but its insertions in the inner wall of the rim remain visible.

*Range*. Late Pliensbachian – Aalenian (Bown and Cooper, 1998; Ferreira et al., 2019).

*Occurrence*. In El Matuasto I, the FO of *Lotharingius barozii* (small specimens) is in the NJT5a subzone of Mattioli and Erba (1999; roughly corresponding to the *spinatum* SAZ) and defines the base of the NJT4c subzone (within the Davoei AZ) according to Ferreira et al. (2019). In the Neuquén Basin, this event was previously reported within the upper part of the *Fanninoceras disciforme* NAZ (time equivalent of the Spinatum SAZ; latest Pliensbachian) (Pérez Panera and Angelozzi, 2015; Angelozzi and Pérez Panera, 2016) and for the upper Lias (Toarcian) (Angelozzi, 1988). We consider the earliest presence of *Lotharingius barozii* in El Matuasto I to match the record from the NJT4c subzone defined by Ferreira et al. (2019). Likewise, this FO approximately correlates with the Davoei–Margaritatus AZ boundary, which defines the transition from the early to late Pliensbachian, representing the earliest occurrence of the *Lotharingius* genus (Ferreira et al., 2019).

*Remarks*. The original (Noël, 1972) and the emended diagnoses (Goy in Goy et al., 1979) are based upon SEM images, and LM pictures are not available. However, the SEM images shown justify an emended diagnosis. The first paper showing both SEM and LM pictures of *Lotharingius barozii* is Bown (1987b). We referred to the latter paper for the identification of this species under LM. We recognized two morphotypes within this taxon. These are small specimens showing four tenuous and nearly straight isogyres (pl. 2, fig. 17), similar to the specimens figured by Bown and Cooper (1998, pl. 4.15, fig. 11). The central-area structures described under SEM are not present under LM, probably because of preservation issues. The second form shows the typical morphology of a well-developed narrow rim and a wide, subrectangular central area spanned by an axial cross-structure (pl. 2, fig. 18) (Mattioli, 1996; Ferreira et al., 2017); this last morphotype is illustrated by Bown (1987b; pl. 15, figs. 4–5). After a careful biometric study, Ferreira et al. (2017) recognize the size increment of the species from the Pliensbachian to the late Toarcian. Hence, the small morphotype occurring in the lower part of our section would represent the earliest and smaller forms of this species. Towards the upper part of El Matuasto I, an abrupt change to the typical, larger morphology is observed. According to Mattioli (1996) and Ferreira et al. (2017) *Lotharingius barozii* is distinguished from the other species of *Lotharingius* by its overall elliptical shape, equidimensional thickness of inner and outer cycles of the distal shield, and its broadly open, oval central area. Bown (1987b) stated that *L. barozii* is closely related to *Bussonius prinsii*. Both species possess a similar placolith and central-area structures. The differences between them are that in *B. prinsii* the outer cycle elements of the distal shield are radially arranged; this feature makes the outer cycle of *B. prinsii* grey in LM, while both cycles are white in *L. barozii*. Also, the buttresses spanning the central area of *B. prinsii* are thicker and more prominent than in *L. barozii*.

Grade "NANNOLITHS" Perch-Nielsen 1985b

Family SCHIZOSPHAERELLACEAE Deflandre, 1959

Genus ***Schizosphaerella*** Deflandre and Dangeard, 1938

*Type species*. *Schizosphaerella punctulata* Deflandre and Dangeard, 1938

***Schizosphaerella punctulata*** Deflandre and Dangeard, 1938

1938 *Schizosphaerella punctulata* Deflandre and Dangeard, pp. 1115–1117, figs. 1–6.
1961 *Nannopatina grandaeva* Stradner, p. 78, text-figs. 1–10 (nomen nudum).
1969 *Nipterula sabina* Farinacci, p. 227; pl. 3, figs. 1–2, text-figs. 1a–b.71
1971 *Schizosphaerella punctulata* Deflandre and Dangeard, 1938. Medd, p. 830, pl. 2, fig. 5.
1972 *Schizosphaerella punctulata* Deflandre and Dangeard, 1938. Noël, pp. 121–122, pl. 15, figs. 2–4.
1977 *Schizosphaerella punctulata* Deflandre and Dangeard, 1938. Hamilton, pl. 1, figs. 1–3; pl. 3, figs. 1–2.
1979 *Schizosphaerella punctulata* Deflandre and Dangeard, 1938. Hamilton, fig. 20.
1979 *Schizosphaerella punctulata* Deflandre and Dangeard, 1938. Moshkovitz, p. 458, pl. 1, figs. 1–10.
1979 *Schizosphaerella astraea* Moshkovitz, pp. 458–459, pl. 2, figs. 1–8.

1982 *Schizosphaerella punctulata* Deflandre and Dangeard, 1938. Hamilton in Lord, pl. 3.1, figs. 17–18; pl. 3.4, figs. 8–9.
1986 *Schizosphaerella punctulata* Deflandre and Dangeard, 1938. Young et al., pl., figs. J, K.
1987b *Schizosphaerella punctulata* Deflandre and Dangeard, 1938. Bown, pp. 76–80, pl. 11, figs. 7–9; pl. 15, figs. 25–26.
1988 *Schizosphaerella punctulata* Deflandre and Dangeard, 1938. Angelozzi, p. 143, pl. 2, figs. 1–2.
1988 *Schizosphaerella punctulata* Deflandre and Dangeard, 1938. Bown et al., pl. 1, fig. 1.
1992 *Schizosphaerella punctulata* Deflandre and Dangeard, 1938. Baldanza and Mattioli, pl. 1, fig. 9.
1994 *Schizosphaerella punctulata* Deflandre and Dangeard, 1938. Goy et al., pl. 7, figs. 13–14.
1998 *Schizosphaerella punctulata* Deflandre and Dangeard, 1938. Bown and Cooper in Bown, pl. 4.8, figs. 18–19; pl. 4.16, figs. 21–22.
1998 *Schizosphaerella* spp. Deflandre and Dangeard, 1938. Parisi et al., pl. 4, fig. 1.
1999 *Schizosphaerella punctulata* Deflandre and Dangeard, 1938. Mattioli and Erba, p. 365, pl. 1, figs. 1–2.
2000 *Schizosphaerella punctulata* Deflandre and Dangeard, 1938. Walsworth-Bell, p. 51, fig. 4.7; p. 90, fig. 6.3.
2007 *Schizosphaerella* spp. Deflandre and Dangeard, 1938. Fraguas et al., pl. 2, fig. 14.
2010 *Schizosphaerella* spp. Deflandre and Dangeard, 1938. Reggiani et al., pp. 2–3, pl. 1, fig. 1.
2017 *Schizosphaerella punctulata* Deflandre and Dangeard, 1938. Peti and Thibault., fig. 3, G–Y.
2019 *Schizosphaerella punctulata* Deflandre and Dangeard, 1938. Menini et al., p. 16, pl. 1, figs. 1,7.
2021 *Schizosphaerella* spp. Deflandre and Dangeard, 1938. Fraguas et al., fig. 9, CM.217.

*Range*. Hettangian–Kimmeridgian (Bown and Cooper, 1998).

*Occurrence*. The record of *Schizosphaerella punctulata* is continuous throughout the studied section, attesting the consistent occurrence of this species in the south-eastern Pacific since the early Pliensbachian. Bown (1987b) noticed this taxon from the Neuquén Basin but stated that the locality was undated. Later, Angelozzi (1988) documented the presence of *Schizosphaerella* in the Toarcian. Bown (1992) considers *S. punctulata* to be a typical Tethyan component and explains its absence in the Pliensbachian of the Neuquén Basin possibly due to ecological limitations that would be overcome in the Toarcian with the opening of the Hispanic Corridor. Afterwards, Angelozzi and Pérez Panera (2016) reported *S. punctulata* in the Neuquén Basin since the early Pliensbachian, and this record is confirmed by the present study.

*Remarks*. This large nannolith is composed of a test of organized calcite crystallites formed by two interlocking subhemispherical valves. The characteristic geometric arrangement of the crystals forming the test of *S. punctulata* is recognized by its granular appearance under LM. Unfortunately, only isolated, broken pieces were recovered in El Matuasto I. Another species of the genus, namely *Schizosphaerella astrea*, is reported in the literature; the only difference between the two species concerns the arrangement of the calcite crystal forming the valve (Moshkovitz, 1979). However, this feature is only recognizable under SEM. For this reason, some authors prefer the use of *Schizosphaerella* spp. when working under LM. Recently, three morphotypes of *Schizosphaerella* with overlapping size ranges and different palaeoecologies were identified (Peti and Thibault, 2017; Peti et al., 2021).

## 5 Discussion

Calcareous nannofossil biostratigraphic studies and improvements of "standard" biozonations for the Early Jurassic are mostly based on sections from the Tethys realm, which from a palaeogeographic point of view represents a very small region. Previous works dealing with the Los Molles Formation (Neuquén Basin, Argentina) only presented a general characterization of the nannofossil assemblages and a broad correlation of nannofossil events with the boreal and Tethys realms (Angelozzi, 1988; Angelozzi and Pérez Panera, 2013, 2016; Pérez Panera and Angelozzi, 2015), without a thorough systematic approach. Nevertheless, the Neuquén Basin offers a unique opportunity to compare the evolutionary history of this group between the south-eastern Pacific Ocean and the classic localities situated in the Northern Hemisphere and may contribute to achieving a more comprehensive global biostratigraphic scheme for the Early Jurassic. However, as demonstrated in this contribution, detailed systematic studies on the Neuquén Basin calcareous nannofossil record need to be carried out before detailed correlations can be established.

### 5.1 Taxonomy

When comparing the nannofossil record of the Los Molles Formation in Argentina with the Tethys nannofossil record, some inconsistencies appeared in the literature concerning some murolith–coccoliths. A careful and extensive examination of the original diagnoses was thus undertaken, along with a revision of the known literature for evaluating the synonymies. Thus, it appeared that *Crepidolithus crucifer* has been cited inconsistently in the literature due to its informal introduction made by Prins (1969) as nomen nudum (Fig. 3). Because Prins (1969) did not provide a diagnosis, the taxon was not formally recognized until the contribution of Rood et al. (1973). Unfortunately, the SEM image presented then for the holotype is a proximal view of the coccolith, which hinders a proper assessment of the species based on central-area

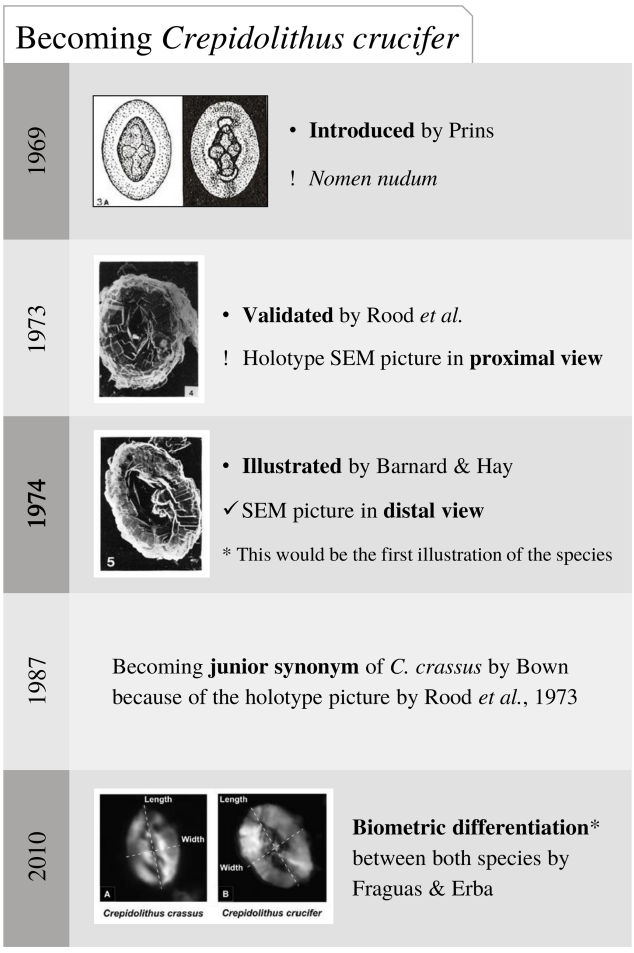


**Figure 3.** Some studied species have a complicated taxonomic history, like *Crepidolithus crucifer*. Images adapted after Prins (1969), Rood et al. (1973), Barnard and Hay (1974), and Fraguas and Erba (2010).

structures that are more clearly visible in distal view. Based on the proximal view features of the holotype, Bown (1987b) established *C. crucifer* as a junior synonym of *C. crassus*. Yet, diverse and sometimes unclear usage of these two names to refer to the same species has been found in the literature for more than 20 years. Fraguas and Erba (2010) differentiated the two taxa by means of biometry and emended the diagnosis of *C. crucifer*. According to this latest description, the SEM picture provided by Barnard and Hay (1974) can actually be considered the first illustration of the species.

*Crepidolithus cavus* was introduced as nomen nudum by Prins (1969) and eventually validated by Rood et al. (1973). Later, Grün et al. (1974) introduced the new species *Crepidolithus impontus* and Goy (in Goy et al., 1979) emended its diagnosis. The *C. impontus* imaged by Grün et al. (1974) resembled *C. cavus* by Prins (1969), and the emendation of *C. impontus* by Goy (1979) better fits with *C. cavus* as described in Rood et al. (1973). Considering these issues, Bown (1987b) tried to clarify the taxonomy of both species, setting *C. impontus* as a junior synonym of *C. cavus*. Nonetheless, the confusion in the literature persisted through time and no consensus about the taxonomic status of these names was reached. In particular, the species with a bridge were assigned to *C. impontus* by some authors, while *C. cavus* was considered for specimens with an empty central area. However, Menini et al. (2019) lumped *C. cavus*–*C. impontus* because the bridge which characterizes *C. impontus* can be broken, although its insertions are generally still visible. After a careful revision, it appears that the holotype of the *C. cavus* SEM image shown by Rood et al. (1973) possesses a relatively narrow central area and a prominent spine. Also, because the SEM image is very poor, sutural lines of the distal shield are not visible, and this specimen resembles a *Parhabdolithus*. A similar interpretation was inferred by Grün et al. (1974) and de Kaenel et al. (1996). Thereby, *C. cavus* in Prins, 1969 ex Rood et al. (1973) should be considered either *P. cavus* or a junior synonym of *P. liasicus* Deflandre, 1952. We support *Crepidolithus impontus* as the correct and valid name because the wide central area may or may not display a central structure according to the preservation quality of the material, but its insertions are still visible. Even if a certain variability in the rim thickness and wideness of central area is observed, the specimens shown in the literature possessing a reduced, narrowly elliptical central area spanned by a spine more likely apply to *Parhabdolithus liasicus*. Recently, Fraguas (2014) described the new species *Crepidolithus cantabriensis*; the diagnosis is, however, incorrect because the cited bicyclic rim extinction pattern does not apply to the genus or the murolith coccoliths. Furthermore, the specimens shown in Fraguas (2014) were taken at 45° under LM crossed polars. Various muroliths display a bicyclic-like extinction pattern at 45°. Accordingly, we assigned some of the *Crepidolithus cantabriensis* figured in Fraguas (2014) to *C. impontus* and some others to *C. crassus* depending on the size of the central area. In fact, Bown (1987b) described a certain variability in the size of the central area of *C. crassus*, which can be vacant, slightly open, or narrower, depending on the size of the distal shield elements.

Bown and Cooper (1998) figured out different-sized morphotypes of *Tubirhabdus patulus*, even though they did not consider these to be subspecies. We recognized three different morphotypes for this species, which are differentiated by a variable central-area shape, besides by their size. Accordingly, we name them "tiny" for the very small, "thick" for those specimens with a thick wall and a very reduced central area, and "thin" for large morphotypes with a large central area in which the hollow tube is well outlined.

Bown (1987) and Bown and Cooper (1998) also described thin and thick *Crepidolithus granulatus* without specifying if these are subspecies or eco-phenotypes. Accordingly, we differentiate these two morphotypes that likely correspond to more or less heavily calcified coccoliths.

A wide morphological variability is described for Early Jurassic murolith–coccoliths, which makes systematic analysis and palaeontology difficult. As biometric studies (e.g. Fraguas and Erba, 2010; Suchéras-Marx et al., 2010) are still scarce, it is difficult to assess if such morphological differences are related to the existence of pseudo-cryptic species, or if they are ecologically driven changes in geometry or calcification. A better understanding of the morphological variability is needed for improving biostratigraphy and also for accurately describing evolutionary patterns.

A quite large morphological variability also occurs within the placolith–coccolith group. Although some biometric studies have been performed on placoliths of Biscutaceae and *Lotharingius* (e.g. Mattioli et al., 2004; Fraguas and Young, 2011; Ferreira et al., 2017), the systematic palaeontology is not yet perfectly established and some morphological species should be revisited, especially within the *Calyculus* and *Similiscutum* groups. Also, we found an inconsistency within the original diagnosis of the *Lotharingius* genus, which comprises several species and dominated the nannofossil assemblages in Toarcian and Aalenian rocks. We propose an emended diagnosis for the genus, which better reflects the morphological characters of the figured holotype, as well as for the type species *L. barozii*.

### 5.2 Biostratigraphy

The calcareous nannofossil assemblage and the species morphology from the studied El Matuasto I section, Los Molles Formation, closely resemble the ones documented in the western Tethys (Fig. 4). The biozonation scheme of Ferreira et al. (2019) was the most suitable for application to the El Matuasto I section. Yet, the Neuquén Basin records several marker species, such as *Biscutum grande*, *Lotharingius barozii*, *Similiscutum finchii*, and the *S. cruciulus* group, allowing good correlation with biostratigraphic schemes established for western Europe. We recorded the *Similiscutum cruciulus* group from the base of the studied section. Bown and Cooper (1998) already considered the FO of the placolith–coccoliths (including *Similiscutum* spp.) to be the major evolutionary event to set the base of the NJT4 zone. Thereby, Ferreira et al. (2019) used the FO of the *Similiscutum cruciulus* group to define the base of the NJT4 zone.

The NJT4a subzone (Mattioli and Erba, 1999 emend. Ferreira et al., 2019) is defined as the interval between the FO of *Similiscutum cruciulus* and the FO of *Biscutum grande*, and it corresponds to the NJ4a subzone of Bown and Cooper (1998) and the NJT4a subzone of Mattioli and Erba (1999). We identified this subzone because of the presence of *S. cruciulus* group from the base of the section until the identification of the ?FO of *B. grande*. Within this subzone, Ferreira et al. (2019) reported the LO of *Crepidolithus timorensis*, but we observed the sporadic presence of this species after the FO of *B. grande*. According to the literature, *Crepidolithus timorensis* has a range restricted to the Sinemurian (Bown and Cooper, 1998) or the lower Pliensbachian (Kristan-Tollman, 1988b), with its LO lying within the NJT4a subzone (Ferreira et al., 2019). The Neuquén Basin record is slightly different because this taxon last occurs within the NJT4b subzone. If not due to reworking (turbidite levels are recorded in the section), this new record constitutes a difference with respect to the Tethyan bioevents, and further analysis in other sections of the Neuquén Basin will help to corroborate the new datum.

The two subsequent NJT4b and NJT4c subzones were easily recognized in the El Matuasto I section. They were defined by Ferreira et al. (2019) as follows: the NJT4b subzone spans the FO of *Biscutum grande* to the FO of *Lotharingius barozii*, and the NJT4c subzone ranges from the FO of *Lotharingius barozii* to the LO of *Parhabdolithus robustus*. Both partly correspond to the NJ4b subzone (Bown and Cooper, 1998) and to the NJT4b subzone (Mattioli and Erba, 1999). Two morphotypes of *Lotharingius barozii* occurred, namely earlier forms with a very thin rim and larger specimens whose features are more consistent with the holotype description. For biostratigraphic purposes, the FO of *Lotharingius barozii* was considered since the occurrence of the earliest forms. This represents the earliest occurrence of the *Lotharingius* genus according to Ferreira et al. (2019).

The FO of *Similiscutum finchii* happens synchronously with the FO of *Lotharingius barozii* classic morphotype within the NJT4c subzone. Within this subzone, the LO of *Crepidolithus pliensbachensis* also occurs. These events perfectly fit the Ferreira et al. (2019) findings in the Lusitanian Basin, Portugal.

*Parhabdolithus robustus* co-occurs with *Crepidolithus impontus* in the upper part of the El Matuasto I section. Such a coexistence is not observed in the north-eastern Pacific (Bown, 1992) or in the boreal (Bown and Cooper, 1998) and Tethys realms (Mattioli and Erba, 1999; Ferreira et al., 2019). Hence, if not related to resedimentation, this co-occurrence may constitute another important difference between the Northern and Southern Hemisphere settings.

### 5.3 Palaeobiogeography

Some species previously considered typical representatives of the Tethys realm were reported for the first time in the Neuquén Basin and in the south-eastern Pacific, such as *Crepidolithus timorensis*, *Mitrolithus elegans*, *Parhabdolithus robustus*, *Similiscutum avitum*, *S. cruciulus*, and *S. orbiculus*. In particular, *Crepidolithus timorensis* is a distinctive component of the assemblages from Timor (south-western Tethys), and its presence in the proto-Atlantic region (Portugal, France) and now in the south-eastern Pacific provides new insights on the species distribution and range. Similarly, *M. elegans* has long been considered a typical component of Tethys assemblages (Bown, 1987b). The similarity observed between the Neuquén Basin and the western Tethyan assemblages is remarkable, especially within

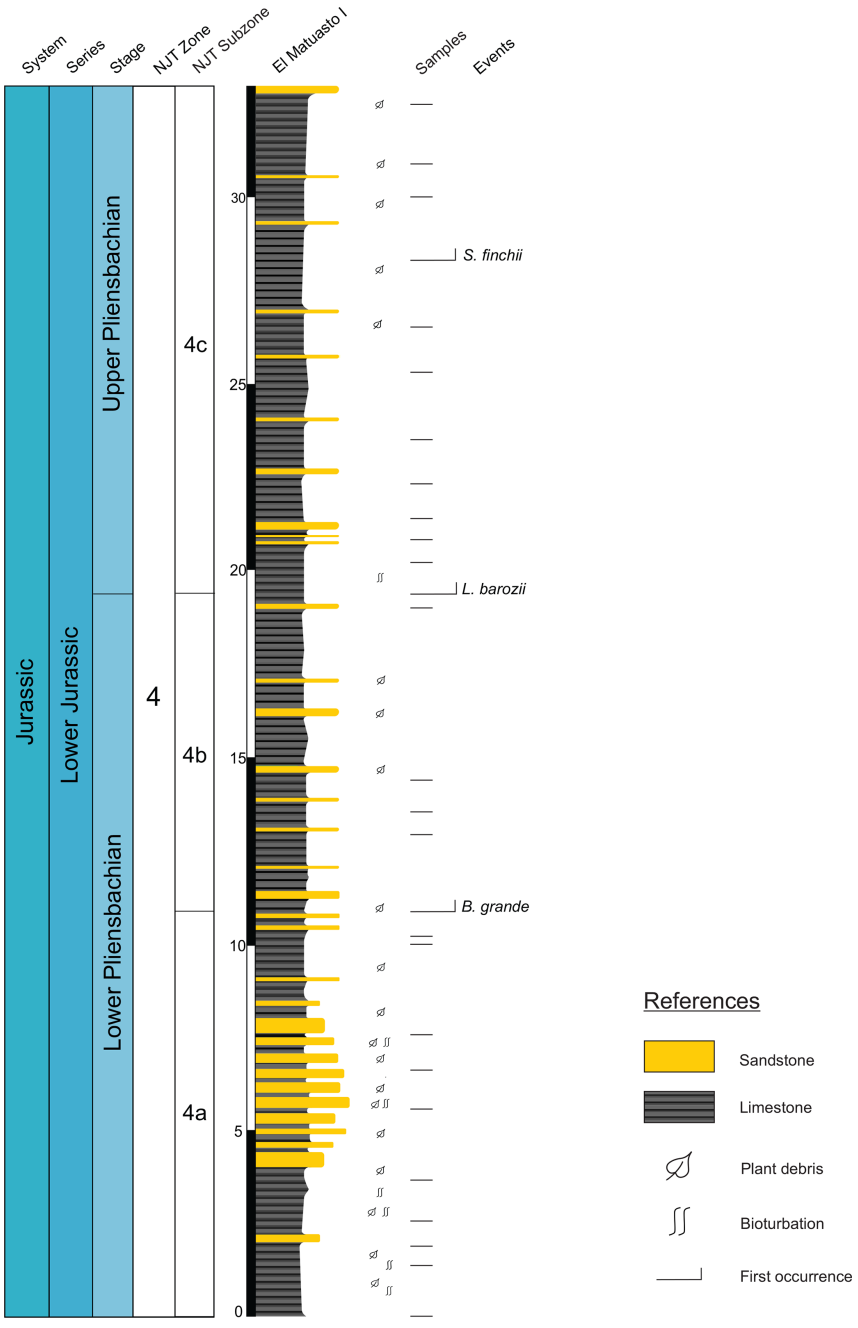


**Figure 4.** Integration of El Matuasto I sedimentary section with the chronostratigraphy, the nannofossil Tethyan zones (NJT; Ferreira et al., 2019), and the main bioevents.

the Lusitanian Basin, Portugal. The assemblage composition, therefore, may suggest the existence of a connection between the Pacific and Tethys oceans since the Pliensbachian (Fig. 1b).

## 6 Conclusions

Although the calcareous nannofossil assemblages from the south-eastern Pacific Ocean has been already described in a few papers (e.g. Bown, 1987b; Al-Suwaidi et al., 2010, 2016; Angelozzi and Pérez Panera, 2013; Fantasia et al., 2018), a thorough taxonomic discussion of the Early Jurassic nannofossil species of the Neuquén Basin is presented for the first time. This contribution settles the taxonomic features of coccoliths recorded in the Neuquén Basin. After the seminal work of Bown (1987b), very little detailed literature exists on coccolith taxonomy. Our review of the existing literature, including very old papers (and species diagnosis in French

or German) and studies published in journals that are difficult to access, revealed some taxonomic inaccuracies, which were propagated in the subsequent literature.

The age of the calcareous nannofossil assemblages recorded in the Los Molles Formation is early Pliensbachian and could be well constrained by applying the Ferreira et al. (2019) zonation conceived for the Lusitanian Basin covering the NJT4a to NJT4c subzones. Considering the limited information on the Lower Jurassic Andean successions, the studied calcareous nannofossils are a valuable contribution to the biostratigraphy of the region. New biostratigraphic data are now available for the Southern Hemisphere, and the global biostratigraphic value of calcareous nannofossils is established.

Many similarities were found between the Neuquén Basin and far locations, particularly within the Lusitanian Basin, Portugal, situated in the proto-Atlantic region. These similarities suggest that a connection between the Neuquén and the Lusitanian basins was established through the Jurassic Hispanic Corridor by the Pliensbachian.

## Appendix A

Alphabetical list of calcareous nannofossil species identified in the present contribution.

*Biscutum grande* Bown, 1987b

*Calyculus* spp. Noël, 1972

*Crepidolithus crassus* (Deflandre in Deflandre and Fert, 1954) Noël, 1965b

*Crepidolithus crucifer* Prins ex Rood et al., 1973 emend. Fraguas and Erba, 2010

*Crepidolithus granulatus* Bown, 1987b

*Crepidolithus impontus* Grün, Prins and Zweili, 1974

*Crepidolithus pliensbachensis* (Crux, 1985) emend. Bown, 1987b

*Crepidolithus timorensis* (Kristan-Tollmann, 1988a) Bown in Bown and Cooper, 1998

*Crucirhabdus primulus* Prins, 1969 ex Rood et al., 1973 emend. Bown, 1987b

Large *Similiscutum* aff. *finchii* (Crux, 1984 emend. Bown, 1987a) de Kaenel and Bergen, 1993

*Lotharingius barozii* Noël, 1972

*Mitrolithus elegans* Deflandre, 1954

*Mitrolithus lenticularis* Bown, 1987b

*Parhabdolithus liasicus* spp. *distinctus* (Deflandre, 1952) Bown, 1987b

*Parhabdolithus liasicus* spp. *liasicus* (Deflandre, 1952) Bown, 1987b

*Parhabdolithus robustus* Noël, 1965b

*Schizosphaerella punctulata* Deflandre and Dangeard, 1938

*Similiscutum avitum* de Kaenel and Bergen, 1993

*Similiscutum cruciulus* de Kaenel and Bergen, 1993

*Similiscutum finchii* (Crux, 1984 emend. Bown, 1987a) de Kaenel and Bergen, 1993

*Similiscutum orbiculus* de Kaenel and Bergen, 1993

*Tubirhabdus patulus* Prins, 1969 ex Rood et al., 1973

**Sample availability.** All the slides containing nannofossils studied and pictured in this contribution are stored in the Y-TEC S.A. Biostratigraphic Laboratory Micropalaeontological Repository (Argentina) with the label YT.RMP_N (Y-TEC Repositorio Micropaleontológico. Nanofósiles) numbers YT.RMP_N.000012.1 to YT.RMP_N.000012.16. The biostratigraphic information is available in Figs. 2 and 4.

**Author contributions.** MCR performed the sampling, sample preparation, and light microscope imaging. The species were determined by MCR under the supervision of the co-authors. The taxonomic descriptions were performed by MCR and EM. MCR prepared the paper and figures with contributions from the co-authors. All authors contributed to writing and editing the article.

**Competing interests.** At least one of the (co-)authors is a member of the editorial board of the *Journal of Micropalaeontology*. The peer-review process was guided by an independent editor, and the authors also have no other competing interests to declare.

**Disclaimer.** Publisher's note: Copernicus Publications remains neutral with regard to jurisdictional claims in published maps and institutional affiliations.

**Acknowledgements.** We would like to thank to the reviewers Ángela Fraguas and Nicolas Thibault for their constructive comments and suggestions to improve the paper, Mateo Gutierrez for helping with the figures, and Gladys Angelozzi for the careful reading of the paper.

**Financial support.** Micaela Chaumeil Rodríguez developed her work in Argentina with funding provided by the Consejo Nacional de Investigaciones Científicas y Técnicas (CONICET). The stay of Micaela Chaumeil Rodríguez at the LGL-TPE (Université Lyon 1, France) was funded by an "Eiffel Excellence Bourse" awarded by the Ministère de l'Europe et des Affaires étrangères through Campus France. Micaela Chaumeil Rodríguez introduced the preparation technique in the Argentinian laboratory with the "Katharina von Salis Graduate Research Fellowship" awarded by the International Nannoplankton Association. This study benefited from the financial support of the Institut Universitaire de France (IUF) to Emanuela Mattioli.

**Review statement.** This paper was edited by Luke Mander and reviewed by Angela Fraguas and Nicolas Thibault.

## References


Aguado, R., O'Dogherty, L., and Sandoval, J.: Fertility changes in surface waters during the Aalenian (mid-Jurassic) of the Western Tethys as revealed by calcareous nannofossils and carbon–cycle perturbations, Mar. Micropaleontol., 68, 268–285, https://doi.org/10.1016/j.marmicro.2008.06.001, 2008.

Al-Suwaidi, A. H., Angelozzi, G. N., Baudin, F., Damborenea, S. E., Hesselbo, S. P., Jenkyns, H. C., Manceñido, M. O., and Riccardi, A. C.: First record of the Early Toarcian Oceanic Anoxic Event from the Southern Hemisphere, Neuquén Basin, Argenina, J. Geol. Soc. Lond., 167, 633–636, https://doi.org/10.1144/0016-76492010-025, 2010.

Al-Suwaidi, A. H., Hesselbo, S. P., Damborenea, S. E., Manceñido, M. O., Jenkyns, H. C., Riccardi, A. C., Angelozzi, G. N., and Baudin, F.: The Toarcian Oceanic Anoxic Event (Early Jurassic) in the Neuquén Basin, Argentina: a reassessment of age and carbon–isotope stratigraphy, J. Geol., 124, 171–193, https://doi.org/10.1086/684831, 2016.

Angelozzi, G. N.: Nanofósiles toarcianos de la Formación Los Molles del perfil Picún–Leufú, Cuenca del Neuquén, República Argentina, 4° Congreso Argentino de Paleontologia y Bioestratigrafía, Mendoza, 1986, Actas, 3, 137–144, 1988.

Angelozzi, G. N. and Pérez Panera, J. P.: Nanofósiles calcáreos del límite Pliensbachiano/Toarciano en la Cuenca Neuquina, Argentina, 5° Simposio Argentino del Jurásico, Trelew, 2013, Abstract, 7, 2013.

Angelozzi, G. N. and Pérez Panera, J. P.: Calcareous nannofossil from Los Molles Formation (Pliensbachian–Aalenian), Neuquén Basin, Argentina, Jurassic Calcareous Nannofossil Workshop, Lyon, 2016, 6–11, 2016.

Angelozzi, G. and Ronchi, D.: Análisis bioestratigráfico del Jurásico Inferior de la Cuenca Neuquina, GEMA SRL, Informe inédito, 1–124, 2002.

Angelozzi, G. N., Damborenea, S. E., Manceñido, M. O., and Riccardi, A. C.: Bioestratigrafía del límite Pliensbachiano–Toarciano en el Arroyo Lapa, Cuenca Neuquina, Argentina, 4° Simposio Argentino del Jurásico y sus límites, Bahía Blanca, 2010, Programa y Resúmenes, 16, 2010.

Arregui, C. A., Carbone, O., and Martínez, R.: El Grupo Cuyo (Jurásico Temprano–Medio) en la Cuenca Neuquina, in: Relatorio 18° Congreso Geológico Argentino: Geología y Recursos Naturales de la provincia del Neuquén, Neuquén, 2011, edited by: Leanza H. A., Arregui, C. A., Carbone, O., Danieli, J. C., and Vallés, J. M., Asociación Geológica Argentina, 77–90, ISBN 978-987-22403-3-2, 2011.

Asgar-Deen, M., Hall, R. L., Craig, J., and Riediger, C.: New biostratigraphic data from the Lower Jurassic Fernie Formation in the subsurface of west-central Alberta and their stratigraphic implications, Can. J. Earth Sci., 40, 45–63, https://doi.org/10.1139/e02-096, 2003.

Baghli, H., Mattioli, E., Spangenberg, J. E., Ruebsam, W., Schwark, L., Bensalah, M., Sebane, A., Pittet, B., Pellenard, P., and Suan, G.: Stratification and productivity in the Western Tethys (NW Algeria) during early Toarcian, Palaeogeogr. Palaeocl., 591, 110864, https://doi.org/10.1016/j.palaeo.2022.110864, 2022.

Baldanza, A. and Mattioli, E.: Biostratigraphical synthesis of nanofossils in the Early Middle Jurassic of southern Tethys, Knihovnicka ZPN, 14a, 111–141, 1992.

Ballent, S. C., Angelozzi, G., and Whatley, R.: Microfósiles calcáreos del Jurásico medio (límite Aaleniano–Bajociano) en el centro oeste de Argentina: consideraciones paleoecológicas y bioestratigráficas, 9° Congreso Geológico Chileno, Puerto Varas, 2000, Resúmenes expandidos, Actas, 1, 432–436, 2000.

Ballent, S., Concheyro, A., Náñez, C., Pujana, I., Lescano, M., Carignano, A., Caramés, A., Angelozzi, G., and Ronchi, D.: Microfósiles mesozoicos y cenozoicos, in: Relatorio del XVIII Congreso Geológico Argentino, Neuquén, 2011, edited by: Leanza, H. A., Arregui, C., Carbone, O., Danieli, J. C., and Vallés, J. M., 489–528, 2011.

Barnard, T. and Hay, W. W.: On Jurassic coccoliths: A tentative zonation of the Jurassic of Southern England and North France, Eclogae Geol. Helv., 67, 563–585, 1974.

Beaufort, L., Barbarin, N., and Gally, Y.: Optical measurements to determine the thickness of calcite crystals and the mass of thin carbonate particles such as coccoliths, Nat. Protoc., 9, 633–642, https://doi.org/10.1038/nprot.2014.028, 2014.

Black, M.: Coccoliths, Endeavour, 24, 131–137, 1965.

Bodin, S., Mattioli, E., Fröhlich, S., Marshall, J. D., Boutib, L., Lahsini, S., and Redfern, J.: Toarcian carbon isotope shifts and nutrient changes from the Northern margin of Gondwana (High Atlas, Morocco, Jurassic): Palaeoenvironmental implications, Palaeogeogr. Palaeocl., 297, 377–390, https://doi.org/10.1016/j.palaeo.2010.08.018, 2010.

Bodin, S., Krencker, F. N., Kothe, T., Hoffmann, R., Mattioli, E., Heimhofer, U., and Kabiri, L.: Perturbation of the carbon cycle during the late Pliensbachian – early Toarcian: New insight from high-resolution carbon isotope records in Morocco, J. Afr. Earth. Sci., 116, 89–104, https://doi.org/10.1016/j.jafrearsci.2015.12.018, 2016.

Bottini, C., Jadoul, F., Rigo, M., Zaffani, M., Artoni, C., and Erba, E.: Calcareous nannofossils at the Triassic/Jurassic boundary: stratigraphic and paleoceanographic characterization, Riv. Ital. Paleontol. S., 122, 141–164, https://doi.org/10.13130/2039-4942/7726, 2016.

Bown, P. R.: The structural development of Early Mesozoic coccoliths and its evolutionary and taxonomic significance, Abh. Geol. B.-A., 39, 33–49, 1987a.

Bown, P. R.: Taxonomy, evolution, and biostratigraphy of Late Triassic–Early Jurassic calcareous nannofossils, Spec. Pap. Palaeontol., 38, 1–118, 1987b.

Bown, P. R.: New calcareous nannofossil taxa from the Jurassic/Cretaceous boundary interval of Sites 765 and 261, Argo Abyssal Plain, in: Proceedings of the Ocean Drilling Program, Scientific Results, 123, 369–379, https://doi.org/10.2973/odp.proc.sr.123.170.1992, 1992.

Bown, P. R. (Ed.): Calcareous nannofossil biostratigraphy, British Micropalaeontological Society Publication Series, Kluwer Academic Publishers, Dordrecht-Boston-London, ISBN 0412-789701, 1998.

Bown, P. R. and Cooper, M. K. E.: Jurassic, in: Calcareous Nannofossil Biostratigraphy, British Micropalaeontological Society Publication Series, edited by: Bown, P. R., Kluwer Academic Publishers, Dordrecht-Boston-London, 34–85, ISBN 0412-789701, 1998.

Bown, P. R. and Ellison, C.: Jurassic–Early Cretaceous nannofossils from the Neuquén Basin, Argentina, J. Nannoplankton Res., 17, 48, 1995.

Bown, P. R. and Lord, A. R.: The occurrence of calcareous nannofossils in the Triassic/Jurassic boundary interval, Cah. Inst. Cath. Lyon, Ser. Sci., 3, 127–136, 1990.

Bown, P. R. and Young, J. R.: Mesozoic calcareous nannoplankton classification, J. Nannoplankton Res., 19, 21–36, 1997.

Bown, P. R., Cooper, M. K. E., and Lord, A. R.: A calcareous nannofossil biozonation scheme for the early to mid Mesozoic, Newsl. Stratigr., 20, 91–114, https://doi.org/10.1127/nos/20/1988/91, 1988.

Braarud, T., Deflandre, G., Halldal, P., and Kamptner, E.: Terminologie, nomenclature et systematique chez les Coccolithophorides, Compte Rendu 8th International Botanical Congress, Paris, 1954, Vol. 17, 69–70, 1955a.

Braarud, T., Deflandre, G., Halldal, P., and Kamptner, E.: Terminology, nomenclature, and systematics of the Coccolithophoridae, Micropaleontology, 1, 157–159, 1955b.

Bucefalo Palliani, R. and Mattioli, E.: High resolution integrated microbiostratigraphy of the Lower Jurassic (late Pliensbachian–early Toarcian) of central Italy, J. Micropalaeontol., 17, 153–172, https://doi.org/10.1144/jm.17.2.153, 1998.

Casadío, S. and Montagna, A.: Estratigrafía de la Cuenca Neuquina, in: Geología de la cuenca Neuquina y sus Sistemas Petroleros, una mirada integradora desde los afloramientos al subsuelo, edited by: Ponce, J. J., Montagna, A., and Carmona, N. B., Fundación YPF (Ciudad Autónoma de Buenos Aires) y Universidad Nacional de Río Negro (Viedma), 8–21, ISBN 978-987-26841-3-6, 2015.

Casellato, C. E. and Erba, E.: Calcareous nannofossil biostratigraphy and paleoceanography of the Toarcian oceanic anoxic event at Colle Di Sogno (southern Alps, northern Italy), Riv. Ital. Paleontol. S., 121, 297–327, https://doi.org/10.13130/2039-4942/6520, 2015.

Cavalier-Smith, T., Allsopp, M. T. E. P., Häuber, M. M., Gothe, G., Chao, E. E., Couch, J. A., and Maier, U. G.: Chromobiote phylogeny: the enigmatic alga Reticulosphaera japonensis is an aberrant haptophyte, not a heterokont, Phycologia, 31, 255-263, https://doi.org/10.1080/09670269600651461, 1996.

Chiari, M., Cobiancchi, M., and Picotti, V.: Integrated stratigraphy (radiolarians and calcareous nannofossils) of the Middle to Upper Jurassic Alpine radiolarites (Lombardian Basin, Italy), Constraints to their genetic interpretation, Palaeogeogr. Palaeocl., 249, 233–270, https://doi.org/10.1016/j.palaeo.2007.02.001, 2007.

Crux, J. A.: Biostratigraphy of Early Jurassic calcareous nannofossils from southwest Germany, N. Jb. Geol. Paläont. Abh., 169, 160–186, 1984.

Crux, J. A.: *Crepidolithus pliensbachensis* nomen novum pro *Crepidolithus ocellatus* Crux 1984 non (Bramlette and Sullivan) Noël 1965, INA Newsl., 7, 31, 1985.

Crux, J. A.: Concerning dimorphism in Early Jurassic coccoliths and the origin of the genus *Discorhabdus* Noël 1965, Abh. Geol. B.-A., 39, 51–55, 1987a.

Crux, J. A.: Early Jurassic calcareous nannofossil biostratigraphic events, Newsl. Stratigr., 17, 79–100, https://doi.org/10.1127/nos/17/1987/79, 1987b.

Cruz, C., Robles, F., Sylwan, C., and Villar, H.: Los sistemas petroleros Jurásicos de la Dorsal de Huincul. Cuenca Neuquina, Argentina. IV Congreso de Exploración y Desarrollo de Hidrocarburos, Mar del Plata, 1999, IAPG, Tomo I, 175–195, 1999.

Cobianchi, M.: Biostratigrafia a nannofossili calcarei del passaggio Domeriano–Toarciano in Val Navezze (Brescia), Atti Tic. Sc. Terra, 33, 127–142, 1990.

Cobianchi, M.: Sinemurian–Early Bajocian calcareous nannofossil biostratigraphy of the Lombardy Basin (Southern Calcareous Alps, northern Italy), Atti Tic. Sc. Terra, 35, 61–106, 1992.

Cobianchi, M. and Picotti, V.: Sedimentary and biological response to sea–level and palaeoceanographic changes of a Lower–Middle Jurassic Tethyan platform margin (Southern Alps, Italy), Palaeogeogr. Palaeocl., 169, 219–244, https://doi.org/10.1016/S0031-0182(01)00217-6, 2001.

da Rocha, R. B., Mattioli, E., Duarte, L., Pittet, B., Elmi, S., Mouterde, R., Cabral, M. C., Comas-Rengifo, M., Gómez, J. J., Goy, A., Hesselbo, S., Jenkyns, H., Littler, K., Mailliot, S., Luiz, C., Oliveira, L. C., Osete, M. L., Perilli, N., Pinto, S., and Suan, G.: Base of the Toarcian Stage of the Lower Jurassic defined by the Global Boundary Stratotype Section and Point (GSSP) at the Peniche section (Portugal), Episodes, 39, 460–481, https://doi.org/10.18814/epiiugs/2016/v39i3/99741, 2016.

de Kaenel, E. and Bergen, J. A.: New Early and Middle Jurassic coccolith taxa and biostratigraphy from the eastern proto–Atlantic (Morocco, Portugal and DSDP Site 547B), Eclogae Geol. Helv., 86, 861–907, 1993.

de Kaenel, E. and Bergen, J. A.: Mesozoic calcareous nannofossil biostratigraphy from sites 897, 899, and 901, Iberia Abyssal Plain: New biostratigraphic evidence, Proceedings of the Ocean Drilling Program, Scientific Results, 149, 27–59, 1996.

de Kaenel, E., Bergen, J. A., and von Salis Perch-Nielsen, K.: Jurassic calcareous nannofossil biostratigraphy of western Europe. Compilation of recent studies and calibration of bioevents, B. Soc. Geol. Fr., 167, 15–28, 1996.

Deflandre, G.: Classe des Coccolithophoridés (Coccolithophoridae. Lohmann, 1902), in: Traité de Zoologie, edited by: Grassé, P. P., Masson, Paris, 439–470, 1952.

Deflandre, G. and Dangeard, L.: *Schizosphaerella*, un nouveau microfossile méconnu du Jurassique moyen et supérieur, C.R. Hebd. Acad. Sci., Paris, 207, 1115–1117, 1938.

Deflandre, G. and Fert, C.: Observations sur les coccolithophoridés actuels et fossiles en microscopie ordinaire et électronique, Ann. Paleontol., 40, 115–176, 1954.

de Vargas, C., Aubry, M. P., Probert, I., and Young, J.: Origin and Evolution of Coccolithophores – From coastal hunters to oceanic farmers, in: Evolution of Primary Producers in the Sea, edited by: Falkowski, P. and Knoll, A., Academic Press, 251–285, https://doi.org/10.1016/B978-0-12-370518-1.X5000-0, 2007.

Dockerill, H. J.: *Triscutum*, a distinctive new coccolith genus from the Jurassic, B. Cent. Rech. Expl., 11, 127–131, 1987.

Edvardsen, B., Eikrem, W., Green, J. C., Andersen, R. A., Moon-van der Staay, S. Y., and Medlin, L. K.: Phylogenetic reconstructions of the Haptophyta inferred from 18S ribosomal DNA sequences and available morphological data, Phycologia, 39, 19–35, https://doi.org/10.2216/i0031-8884-39-1-19.1, 2000.

Fantasia, A., Föllmi, K. B., Adatte, T., Bernárdez, E., Spangenberg, J. E., and Mattioli, E.: The Toarcian Oceanic Anoxic Event in southwestern Gondwana – An example from the Andean Basin, northern Chile, J. Geol. Soc. Lond., 175, 883–902, https://doi.org/10.1144/jgs2018-008, 2018.

Farinacci, A.: The smallest planktonic calcareous forms of Jurassic micrites, in: Proceedings of the First International Conference on

Planktonic Microfossils, Geneva 1967, edited by: Bronnimann, P. and Renz, H. H., E. J. Brill, Leiden, 224–228, 1969.

Fatela, F. and Taborda, R.: Confidence limits of species proportions in microfossil assemblages, Mar. Micropaleontol., 45, 169–174, https://doi.org/10.1016/S0377-8398(02)00021-X, 2002.

Ferreira, J., Mattioli, E., and van de Schootbrugge, B.: Palaeoenvironmental vs. evolutionary control on size variation of coccoliths across the Lower–Middle Jurassic, Palaeogeogr. Palaeocl., 465, 177–192, https://doi.org/10.1016/j.palaeo.2016.10.029, 2017.

Ferreira, J., Mattioli, E., Suchéras-Marx, B., Giraud, F., Duarte, L., Pittet, B., Suan, G., Hassler, A., and Spangenberg, J. E.: Western Tethys Early and Middle Jurassic calcareous nannofossil biostratigraphy, Earth-Sci. Rev., 197, 1–19, https://doi.org/10.1016/j.earscirev.2019.102908, 2019.

Fraguas, A.: *Crepidolithus cantabriensis* nov. sp., a new calcareous nannofossil (Prymnesiophyceae) from the Lower Jurassic of northern Spain, Geobios, 47, 31–38, https://doi.org/10.1016/j.geobios.2013.10.004, 2014.

Fraguas, A. and Erba, E.: Biometric analyses as a tool for the differentiation of two coccolith species of the genus *Crepidolithus* (Pliensbachian, Lower Jurassic) in the Basque-Cantabrian Basin (Northern Spain), Mar. Micropaleontol., 77, 125–136, https://doi.org/10.1016/j.marmicro.2010.08.004, 2010.

Fraguas, A. and Young, J. R.: Evolution of the coccolith genus *Lotharingius* during the Late Pliensbachian–Early Toarcian interval in Asturias (N Spain) – Consequences of the Early Toarcian environmental perturbations, Geobios, 44, 361–375, https://doi.org/10.1016/j.geobios.2010.10.005, 2011.

Fraguas, A., Comas-Rengifo, M. J., and Perilli, N.: Los nanofósiles calcáreos del Pliensbachiense de la sección de Tudanca (Cuenca Vasco–Cantábrica, España), Coloquios Paleontol., 57, 225–269, 2007.

Fraguas, A., Comas-Rengifo, M. J., and Perilli, N.: Pliensbachian calcareous nannofossils of the Santotis section (Basque–Cantabrian Basin, N Spain), Atti Soc. Tosc. Sci. Nat. Mem. Serie A, 113, 49–56, 2008.

Fraguas, A., Herrle, J. O., Pross, J., and van de Schootbrugge, B.: Biostratigraphy of Lower Jurassic calcareous nannofossils from the Schandelah core (NW Germany), INA14 abstracts, Reston, Virginia, USA, 2013, J. Nannoplankton Res., Spec. Issue, 57, 2013.

Fraguas, A., Comas-Rengifo, M. J., and Perilli, N.: Calcareous nannofossil biostratigraphy of the Lower Jurassic in the Cantabrian Range (Northern Spain), Newsl. Stratigr., 48, 179–199, https://doi.org/10.1127/nos/2015/0059, 2015.

Fraguas, A., Comas-Rengifo, M. J., Goy, A., and Gómez, J. J.: Upper Sinemurian-Pliensbachian calcareous nannofossil biostratigraphy of the E Rodiles section (Asturias, N Spain), A reference section for the connection between the Boreal and Tethyan Realms, Newsl. Stratigr., 51, 227–244, https://doi.org/10.1127/nos/2017/0401, 2018.

Fraguas, A., Gómez, J. J., Goy, A., and Comas-Rengifo, M. J.: The response of calcareous nannoplankton to the latest Pliensbachian-early Toarcian environmental changes in the Camino section (Basque-Cantabrian Basin, North Spain), Geol. Soc. Lond. Spec. Publ., 514, 31–58, https://doi.org/10.1144/SP514-2020-256, 2021.

Gardin, S. and Manivit, H.: Biostratigraphie des nannofossiles calcaires du Toarcien du Quercy (Sud-Ouest de la France) – Comparaison avec la coupe stratotypique de la cimenterie d'Airvault (Deux-Sèvres, France), Geobios, 27, 229–244, https://doi.org/10.1016/S0016-6995(94)80142-8, 1994.

Goy, A., Ureta, S., Arias, C, Canales, M. L., García Joral, F., Herrero, C., Martinez, G., and Perilli, N.: The Fuentelsaz section (Iberian range, Spain), a possible Stratotype for the base of the Aalenian Stage, Misc. Serv. Geol. Naz., 5, 1–31, 1994.

Goy, G.: Nannofossiles calcaries des schistes carton (Toarcien Inférieur) du Basin de Paris, Documents de la RCP 459 (1), CNRS, Paris, 86 pp., ISBN 2903-606005, 1981.

Goy, G., Noël, D., and Busson, G.: Les conditions de sédimentation des schistes-carton (Toarcien inf.) du bassin de Paris déduites de l'étude des nannofossiles calcaires et des diagraphies, Docum. Lab. Géol. Fac. Sci. Lyon, 75, 33–57, 1979.

Gradstein, F. M., Ogg, J. G., Schmitz, M., and Ogg, G.: The Geological Time Scale 2012, Elsevier, 1176 pp., https://doi.org/10.1016/C2011-1-08249-8, 2012.

Groeber, P.: Estratigrafía del Dogger en la República Argentina, Estudio sintético comparativo, Dir. Gral. Minas, Geol. e Hidrogeología, Bol. 18 Serie B (Geología), 1–81, 1918.

Grün, W., Prins, P., and Zweili, F.: Coccolithophoriden aus dem Lias epsilon von Holzmaden (Deutschland), N. Jb. Geol. Paläont. Abh., 147, 294–328, 1974.

Gulisano, C. A. and Gutiérrez Pleimling, A.: Field Guide, The Jurassic of the Neuquén Basin, Neuquén Province, Asociación Geológica Argentina, Serie E, 2, 1–111, 1995.

Gulisano, C. A., Gutiérrez Pleimling, A. R., and Digregorio, R. E.: Esquema estratigráfico de la secuencia jurásica del oeste de la provincia del Neuquén, IX Congreso Geológico Argentino, S. C. Bariloche, 1984, Actas I, 236–259, 1984.

Gutiérrez Pleimling, A. R., Ambrosio, A., Gómez, C., Bustos, G., González, J. M., Guzmán, C., and Tapia, F.: Sequence-stratigraphic study of Cuyo Group in the Agua del Cajón Block, Neuquén Basin, Argentina, J. S. Am. Earth Sci., 110, 103373, https://doi.org/10.1016/j.jsames.2021.103373, 2021.

Hamilton, G. B.: Early Jurassic calcareous nannofossils from Portugal and their biostratigraphic use, Eclogae Geol. Helv., 70, 575–597, 1977.

Hamilton, G. B.: A biostratigraphic study of Jurassic calcareous nannofossils from Portugal and Great Britain, PhD thesis, University College London, England, 261 pp., 1978.

Hamilton, G. B.: Lower and Middle Jurassic calcareous nannofossils from Portugal, Eclogae Geol. Helv., 72, 1–17, 1979.

Hamilton, G. B.: Triassic and Jurassic calcareous nannofossils, in: A Stratigraphical Index of Calcareous Nannofossils, edited by: Lord, A. R., British Micropalaeontological Society Series, Ellis Horwood, Chichester, 17–39, 1982.

Howell, J. A., Schwarz, E., Spalletti, L. A., and Veiga, G. D.: The Neuquén Basin: an overview, Geol. Soc. Lond. Spec. Publ., 252, 1–14, https://doi.org/10.1144/GSL.SP.2005.252.01.01, 2005.

Kristan-Tollmann, E.: Coccolithen aus den Älteren Allgäuschichten (Alpiner Lias, Sinemur) von Timor, Indonesien, Geol. Paläont. Mitt. Innsbruck, 15, 71–83, 1988a.

Kristan-Tollmann, E.: Coccolithen aus dem Pliensbach (Ältere Allgäuschichten) von Timor, Indonesien, Geol. Paläont. Mitt. Innsbruck, 15, 109–133, 1988b.

Lanés, S.: Late Triassic to Early Jurassic sedimentation in northern Neuquén Basin, Argentina, Tectosedimentary Evo-

lution of the First Transgression, Geol. Acta, 3, 81–106, https://doi.org/10.1344/105.000001399, 2005.

Leanza, H. A.: Las principales discordancias del Mesozoico de la Cuenca Neuquina según observaciones de superficie, Rev. Mus. Argent. Cienc. Nat., 11, 145–184, 2009.

Legarreta, L. and Gulisano, C. A.: Análisis estratigráfico secuencial de la Cuenca Neuquina (Triásico superior–Terciario inferior), in: Cuencas Sedimentarias Argentinas, Serie Correlación Geológica, edited by: Chebli, G. and Spalletti, L., INSUGEO, S. M. Tucumán, 6, 221–243, 1989.

Legarreta, L. and Uliana, M. A.: The Jurassic succession in West-Central Argentina, stratal patterns, sequences and paleogeographic evolution, Palaeogeogr. Palaeocl., 120, 303–330, https://doi.org/10.1016/0031-0182(95)00042-9, 1996.

Legarreta, L. and Uliana, M. A.: El Jurásico y Cretácico de la Cordillera Principal y la Cuenca Neuquina. Facies sedimentarias, in: Geología Argentina, Anales 29, edited by: Caminos, R. L., Serv. Geol. Min. Arg., Buenos Aires, 339–416, 1999.

Legarreta, L. and Villar, H.: Las facies generadoras de hidrocarburos de la Cuenca Neuquina, Petrotecnia, 53, 14–42, 2012.

López-Otálvaro, G. E., Suchéras-Marx, B., Giraud, F., Mattioli, E., and Lécuyer, C.: *Discorhabdus* as a key coccolith genus for paleoenvironmental reconstructions (Middle Jurassic, Lusitanian Basin) – Biometry and taxonomic status, Mar. Micropaleontol., 94–95, 45–57, https://doi.org/10.1016/j.marmicro.2012.06.003, 2012.

Lozar, F.: Calcareous nannofossil biostratigraphy of Lower Liassic from Western Tethys, Palaeontogr. Italica, 82, 91–121, 1995.

Mailliot, S.: Production carbonate pelagique par les nannofossils calcaires au cours de l'evenement anoxique du Toarcien Inferieur, PhD thesis, Université Claude Bernard Lyon 1, France, 315 pp., 2006.

Mailliot, S., Mattioli, E., Guex, J., and Pittet, B.: The Early Toarcian anoxia, a synchronous event in the Western Tethys? An approach by quantitative biochronology (Unitary Associations) applied on calcareous nannofossils, Palaeogeogr. Palaeocl., 240, 562–586, https://doi.org/10.1016/j.palaeo.2006.02.016, 2006.

Mattioli, E.: New calcareous nannofossil species from the Early Jurassic of Tethys, Riv. Ital. Paleontol. S., 102, 397–412, https://doi.org/10.13130/2039-4942/5274, 1996.

Mattioli, E. and Erba, E.: Synthesis of calcareous nannofossil events in Tethyan lower and middle Jurassic successions, Riv. Ital. Paleontol. S., 105, 343–376, https://doi.org/10.13130/2039-4942/5380, 1999.

Mattioli, E. and Pittet, B.: Spatial and temporal distribution of calcareous nannofossils along a proximal–distal transect in the Lower Jurassic of the Umbria–Marche Basin (central Italy), Palaeogeogr. Palaeocl., 205, 295–316, https://doi.org/10.1016/j.palaeo.2003.12.013, 2004.

Mattioli, E., Pittet, B., Young, J. R., and Bown, P. R.: Biometric analysis of Pliensbachian–Toarcian (Lower Jurassic) coccoliths of the family Biscutaceae, intra- and interspecific variability versus palaeoenvironmental influence, in: Calcareous Nannofossil Palaeoecology and Palaeocenographic Reconstructions, Proceedings of the INA9 conference, Parma 2002, edited by: Villa, G., Lees, J. A., and Bown, P. R., Mar. Micropaleontol., 52, 5–27, https://doi.org/10.1016/j.marmicro.2004.04.004, 2004.

Mattioli, E., Plancq, J., Boussaha, M., Duarte, L. V., and Pittet, B.: Calcareous nannofossil biostratigraphy, new data from the Lower Jurassic of the Lusitanian Basin, Comun. Geol., 100, 69–76, 2013.

Medd, A. W.: Some Middle and Upper Jurassic Coccolithophoridae from England and France, in: Proceedings of the Second Planktonic Conference Roma 1970, edited by: Farinacci, A., Edizioni Tecnoscienza, Rome, 2, 821–844, 1971.

Medd, A. W.: The Upper Jurassic coccoliths from the Haddenham and Gamlingay boreholes (Cambridgeshire, England), Eclogae Geol. Helv., 72, 19–109, 1979.

Menini, A., Mattioli, E., Spangenberg, J. E., Pittet, B., and Suan, G.: New calcareous nannofossil and carbon isotope data for the Pliensbachian/Toarcian boundary (Early Jurassic) in the western Tethys and their paleoenvironmental implications, Newsl. Stratigr., 52, 173–196, https://doi.org/10.1127/nos/2018/0476, 2019.

Menini, A., Mattioli, E., Hesselbo, S. P., Ruhl, M., and Suan, G.: Primary versus carbonate production in the Toarcian, a case study from the Llanbedr (Mochras Farm) borehole, Wales, Geol. Soc. Lond. Spec. Publ., 514, 59–81, https://doi.org/10.1144/SP514-2021-19, 2021.

Mercuzot, M., Pellenard, P., Durlet, C., Bougeault, C., Meister, C., Dommergues, J. L., Thibault, N., Baudin, F., Mathieu, O., Bruneau, L., Huret, E., and El Hmidi, K.: Carbon-isotope events during the pliensbachian (Lower jurassic) on the African and European margins of the nw tethyan realm, Newsl. Stratigr., 53, 41–69, https://doi.org/10.1127/nos/2019/0502, 2019.

Moshkovitz, S.: On the distribution of *Schizosphaerella punctulata* Deflandre and Deflandre Rigaud and *Schizosphaerella atsraea* n. sp. in the Liassic section of Stowell Park Borehole (Gluoucestershire) and in some other Jurassic localities of England, Eclogae Geol. Helv., 72, 455–465, 1979.

Nini, C., Baldanza, A., and Nocchi, M.: Late Domerian–Toarcian calcareous nannofossil biostratigraphy, benthic foraminiferal assemblages and their paleoenvironmental implications – Montebibico area (Spoleto, Central Italy), Rev. Paleobiol., 14, 271–319, 1995.

Noël, D.: Note préliminaire sur des Coccolithes jurassiques, Cah. de Micropaléo., 1, 1–12, 1965a.

Noël, D.: Sur les coccolithes du Jurassique européen et d'Afrique du Nord. Essai de classification des coccolithes fossils, PhD thesis, Editions du C.N.R.S, Paris, 260 pp., 1965b.

Noël, D.: Nannofossiles calcaires de sédiments jurassiques finement laminés, B. Mus. Natl. Hist. Nat., 75, 95–156, 1972.

Parisi, G., Baldanza, A., Benedetti, L., Mattioli, E., Venturi, F., and Cresta, S.: Toarcian stratigraphy of the Colle d'Orlando section (Umbria, Central Italy, northern Apennine), B. Soc. Paleontol. Ital., 37, 3–39, 1998.

Perch-Nielsen, K.: Mesozoic calcareous nannofossils, in: Plankton Stratigraphy, edited by: Bolli, H. M., Saunders, J. B., and Perch-Nielsen, K., Cambridge University Press, Cambridge, 329–426, ISBN 0521-23576-6, 1985a.

Perch-Nielsen, K.: Cenozoic calcareous nannofossils, in: Plankton Stratigraphy, edited by: Bolli, H. M., Saunders, J. B., and Perch-Nielsen, K., Cambridge University Press, Cambridge, 427–554, ISBN 0521-23576-6, 1985b.

Pérez Panera, J. P. and Angelozzi, G.: Pliensbachian/Toarcian Calcareous nannofossil events in the Los Molles Formation, Neuquen Basin, Argentina, 15th International Nannoplankton Association Meeting, Philippines, 2015, 68, 2015.

Perilli, N.: Calibration of early–middle Toarcian nannofossil events based on high-resolution ammonite biostratigraphy in two expanded sections from the Iberian Range (East Spain), Mar. Micropaleontol., 39, 293–308, https://doi.org/10.1016/S0377-8398(00)00025-6, 2000.

Perilli, N. and Comas-Rengifo, M. J.: Calibration of Pliensbachian calcareous nannofossil events in two ammonite-controlled sections from Northern Spain (Basque–Cantabrian area), Riv. Ital. Paleontol. S., 108, 133–152, https://doi.org/10.13130/2039-4942/5463, 2002.

Perilli, N. and Duarte, L. V.: Toarcian nannobiohorizons from Lusitanian Basin (Portugal) and their calibration against ammonite zones, Riv. Ital. Paleontol. S., 112, 417–434, https://doi.org/10.13130/2039-4942/6350, 2006.

Perilli, N., Fraguas, A., and Comas-Rengifo, M. J.: Reproducibility and reliability of the Pliensbachian calcareous nannofossil biohorizons from the Basque–Cantabrian Basin (Northern Spain), Geobios, 43, 77–85, https://doi.org/10.1016/j.geobios.2009.06.009, 2010.

Peti, L. and Thibault, N.: Abundance and size changes in the calcareous nannofossil Schizosphaerella – Relation to sea-level, the carbonate factory and palaeoenvironmental change from the Sinemurian to earliest Toarcian of the Paris Basin, Palaeogeogr. Palaeocl., 485, 271–282, https://doi.org/10.1016/j.palaeo.2017.06.019, 2017.

Peti, L., Thibault, N., Clemence, M. E., Korte, C., Dommergues, J. L., Bougeault, C., Pellenard, P., Jelby, M. E., and Ullmann, C. V.: Sinemurian–Pliensbachian calcareous nannofossil biostratigraphy and organic carbon isotope stratigraphy in the Paris Basin, Calibration to the ammonite biozonation of NW Europe, Palaeogeogr. Palaeocl., 468, 142–161, https://doi.org/10.1016/j.palaeo.2016.12.004, 2017.

Peti, L., Thibault, N., Korte, C., Ullmann, C. V., Cachão, M., and Fibæk, M.: Environmental drivers of size changes in lower Jurassic *Schizosphaerella* spp., Mar. Micropaleontol., 168, 102053, https://doi.org/10.1016/j.marmicro.2021.102053, 2021.

Picotti, V. and Cobianchi, M.: Jurassic periplatform sequences of the eastern Lombardian Basin (Southern Alps), the deep–sea record of the tectonic evolution, growth and demise history of a carbonate platform, Mem. Sc. Geol. Padova, 48, 171–219, 1996.

Plancq, J., Mattioli, E., Pittet, B., Baudin, F., Duarte, L. V., Boussaha, M., and Grossi, V.: A calcareous nannofossil and organic geochemical study of marine palaeoenvironmental changes across the Sinemurian/Pliensbachian (early Jurassic, ∼ 191 Ma) in Portugal, Palaeogeogr. Palaeocl., 449, 1–12, https://doi.org/10.1016/j.palaeo.2016.02.009, 2016.

Prins, B.: Evolution and stratigraphy of cocolithinids from the Lower and Middle Lias, in: Proceedings of the First International Conference on Planktonic Microfossils, Geneva 1967, edited by: Bronnimann, P. and Renz, H. H., E. J. Brill, Leiden, 547–558, 1969.

Prins, B. and Driel, J. A. M.: Are the nannofloral successions in the Early Jurassic of Western Europe related to geological events?, INA Newsl., 9, 59–60, 1987.

Rai, J. and Jain, S.: Pliensbachian nannofossils from Kachchh, Implications on the earliest Jurassic transgressive event on the western Indian margin, Zitteliana, A 53, 105–120, 2013.

Rai, J., Bajpai, S., Kumar, R., Singh, A., Kumar, K., and Prakash, N.: The earliest marine transgression in western India, new insights from calcareous nannofossils from Lathi Formation, Jaisalmer Basin, Curr. Sci. India, 111, 1631–1639, https://www.jstor.org/stable/24909403 (last access: 16 November 2021), 2016.

Reale, V., Baldanza, A., Monechi, S., and Mattioli, E.: Calcareous nannofossil biostratigraphic events from the Early–Middle Jurassic sequences of the Umbria–Marche area (Central Italy), Mem. Sc. Geol. Padova, 43, 41–75, 1992.

Reggiani, L., Mattioli, E., and Pittet, B.: Spatial distribution of Late Pliensbachian (Early Jurassic) calcareous nannofossils within the Lusitanian basin (Portugal), Geobios, 43, 87–97, https://doi.org/10.1016/j.geobios.2009.06.005, 2010.

Reolid, M., Mattioli, E., Nieto, L. M., and Rodríguez-Tovar, F. J.: The Early Toarcian Oceanic Anoxic Event in the External Subbetic (Southiberian Palaeomargin, Westernmost Tethys) – Geochemistry, nannofossils and ichnology, Palaeogeogr. Palaeocl., 411, 79–94, https://doi.org/10.1016/j.palaeo.2014.06.023, 2014.

Riccardi, A. C.: The Jurassic of Argentina and Chile, in: The Phanerozoic Geology of the World II. The Mesozoic, 8, edited by: Moullade, M. and Nairn, A. E. M., Elsevier Scientific Publications B.V., 201–263, ISBN 978-0-44441-671-1, 1983.

Riccardi, A. C.: El Jurásico de la Argentina y sus amonites, Rev. Asoc. Geol. Argent., 63, 625–643, 2008a.

Riccardi, A. C.: The marine Jurassic of Argentina, a biostratigraphic framework, Episodes, 31, 326–335, https://doi.org/10.18814/epiiugs/2008/v31i3/007, 2008b.

Riccardi, A. C. and Gulisano, C. A.: Unidades limitadas por discontinuidades. Su aplicación al Jurásico andino, Rev. Asoc. Geol. Argent., 45, 346–364, 1990.

Riccardi, A. C., Damborenea, S. E., Manceñido, M. O., and Ballent, S. C.: Hettangiano y Sinemuriano marinos en Argentina, Actas V Congr. Geol. Chileno, 2, 359–374, 1988.

Riccardi, A. C., Damborenea, S. E., Manceñido, M. O., and Ballent, S. C.: Hettangian and Sinemurian (Lower Jurassic) biostratigraphy of Argentina, J. South Am. Earth Sci., 4, 159–170, https://doi.org/10.1016/0895-9811(91)90028-J, 1991.

Rood, A. P. and Barnard, T.: On Jurassic coccoliths, *Stephanolithion*, *Diadozygus* and related genera, Eclogae Geol. Helv., 65, 327–342, 1972.

Rood, A. P., Hay, W. W., and Barnard, T.: Electron Microscope Studies of Oxford Clay Coccoliths, Eclogae Geol. Helv., 64, 245–272, 1971.

Rood, A. P., Hay, W. W., and Barnard, T.: Electron microscope studies of Lower and Middle Jurassic coccoliths, Eclogae Geol. Helv., 66, 365–382, 1973.

Roth, P. H.: Preservation of calcareous nannofossils and fine-grained carbonate particles in mid-Cretaceous sediments from the southern Angola Basin, site 530, Initial Reports of the Deep Sea Drilling Project, edited by: Amidei, R., 75, US Government Printing Office, 651–655, https://doi.org/10.2973/dsdp.proc.75.112.1984, 1984.

Sales, T., Giusiano, A., and Tunik, M.: Análisis preliminar del potencial como shale oil que presenta la Formación Los Molles (Miembro Pelítico Inferior) en el depocentro Barda Colorada Este, zona de la Dorsal de Huincul, Cuenca Neuquina, IX Congreso de Exploración y Desarrollo de Hidrocarburos, Abstracts Extendidos, 203–210, 2014.

Sandoval, J., Bill, M., Aguado, R., O'Dogherty, L., Rivas, P., Morard, A., and Guex, J.: The Toarcian in the Subbetic basin

(southern Spain), Bio-events (ammonite and calcareous nannofossils) and carbon–isotope stratigraphy, Palaeogeogr. Palaeocl., 342–343, 40–63, https://doi.org/10.1016/j.palaeo.2012.04.028, 2012.

Spalletti, L. A., Parent, H., Veiga, G. D., and Schwarz, E.: Ammonites and biostratigraphy of the Cuyo Group in the Sierra de Reyes (central Neuquén Basin, Argentina) and their sequential significance, Andean Geol., 39, 464–481, https://doi.org/10.5027/andgeoV39n3-a06, 2012.

Suchéras-Marx, B., Mattioli, E., Pittet, B., Escarguel, G., and Suan, G.: Astronomically paced coccolith size variations during the early Pliensbachian (Early Jurassic), Palaeogeogr. Palaeocl., 295, 281–292, https://doi.org/10.1016/j.palaeo.2010.06.006, 2010.

Stipanicic, P. N.: El avance en los conocimientos del Jurásico argentino a partir del esquema de Groeber, Rev. Asoc. Geol. Argent., 24, 367–388, 1969.

Stoico, M. and Baldanza, A.: Early and middle Jurassic calcareous nannofossil biozonation of the Monti Sabini area (Latium, Norhern Apennines, Central Italy), Palaeopelagos, 5, 75–110, 1995.

Stradner, H.: Vorkommen von Nannofossilien im Mesozoikum und Alttertiär, Erdöl-Zeitschrift, 77, 77–88, 1961.

Stradner, H.: New contributions to Mesozoic stratigraphy by means of nannofossils, in: Proceedings of the Sixth World Petroleum Congress, Frankfurt am Main, Germany, 1963, Section 1 Paper 4, 167–183, 1963.

Tremolada, F., van de Schootbrugge, B., and Erba, E.: The Early Jurassic Schizosphaerellid crisis, implications for calcification rates and phytoplankton evolution across the Toarcian OAE in Cantabria, Spain, Paleoceanography, 20, PA2011, https://doi.org/10.1029/2004PA001120, 2005.

Turland, N. J., Wiersema, J. H., Barrie, F. R., Greuter, W., Hawksworth, D. L., Herendeen, P. S., Knapp, S., Kusber, W.-H., Li, D.-Z., Marhold, K., May, T. W., McNeill, J., Monro, A. M., Prado, J., Price, M. J., and Smith, G. F.: International Code of Nomenclature for algae, fungi, and plants (Shenzhen Code) adopted by the Nineteenth International Botanical Congress Shenzhen, China, July 2017, Regnum Vegetabile 159, Glashütten, Koeltz Botanical Books, https://doi.org/10.12705/Code.2018, 2018.

Varol, O. and Girgis, M.: New taxa and taxonomy of some Jurassic to Cretaceous calcareous nannofossils, Neues. Jahrb. Geol. P.-A., 192, 221–253, 1994.

Veiga, G. D., Spalletti, L. A., and Schwarz, E.: Esquema estratigráfico secuencial de alta resolución para los depósitos del Jurásico Inferior a Medio (Grupo Cuyo) en el sector central de la Cuenca Neuquina, Integración de información de afloramientos y subsuelo, Congreso Geológico Chileno, Santiago, 2009, Vol. 12, 2009.

Veiga de Oliveira, L. C., Dino, R., Duarte, L. V., and Perilli, N.: Calcareous nannofossils and palynomorphs from Pliensbachian–Toarcian boundary in Lusitanian Basin, Portugal, Rev. Bras. Paleontol., 10, 5–16, 2007a.

Veiga de Oliveira, L. C., Perilli, N., and Duarte, L. V.: Calcareous nannofossil assemblages around the Pliensbachian/Toarcian boundary in the reference section of Peniche (Portugal), Ciências da Terra (UNL), 45, 45–50, 2007b.

Vergani, G. D., Tankard, A. J., Belotti, H. J., and Welsink, H. J.: Tectonic evolution and paleogeography of the Neuquén Basin, Argentina, Petroleum Basins of South America, Am. Assoc. Petr. Geol. Mem., 62, 383–402, 1995.

Vergani, G. Angelozzi, G., and Ronchi, D.: Análisis bioestratigráfico del Jurásico Inferior en la Dorsal de Huincul, Cuenca Neuquina, in: Resúmenes del 1° Simposio Argentino del Jurásico, La Plata, 2003, Ameghiniana, 40, 46R–47R, 2003.

Walsworth-Bell, E. B.: Jurassic calcareous nannofossils and environmental cycles, PhD thesis, University College London, England, 137 pp., 2000.

Weaver, C. E.: Paleontology of the Jurassic and Cretaceous of West Central Argentina, Univ. Washington, Memoir, 1, 469 pp., 1931.

Young, J. R.: Report – terminology working group meeting, London April 1992, INA Newsl., 14, 6–8, 1992.

Young, J. R. and Bown, P. R.: Proposals for a revised classification system for calcareous nannoplankton, J. Nannoplankton Res., 19, 15–47, 1997.

Young, J. R., Teale, C. T., and Bown, P. R.: Revision of the stratigraphy of the Longobucco Group (Liassic, southern Italy), based on new data from nannofossils and ammonites, Eclogae Geol. Helv., 79, 117–135, 1986.